Double-scattering correction for the critical dynamics of a classical fluid

Richard A. Ferrell and Jayanta K. Bhattacharjee
Institute for Physical Science and Technology and Department of Physics and Astronomy, University of Maryland, College Park, Maryland 20742
(Received 27 March 1978; revised manuscript received 3 August 1978)

It is found that light undergoing double scattering in a fluid introduces a spurious curvature in the semilog plot of the time-dependent correlation function versus time. The amount of curvature to be expected is calculated as a function of the parameters of the experiment. This permits the correction of experimental data by the subtraction of the double-scattering contribution. Alternatively, we express the results of our calculation in frequency space by exhibiting the deviation to be expected from a Lorentzian spectrum. A further description of the double scattering is given in terms of a continuous distribution of relaxation rates. Also included, as a by-product, is a brief treatment of the double-scattering correction for the equal-time correlation function. Small-angle approximations, valid in the extreme critical region, lead to analytic results which are found to be in good agreement with numerical computations of Bray and Chang. As in their work, our calculations are limited to the 90° scattering geometry.

I. INTRODUCTION

A. Organization

With the steady increase in accuracy of experiments studying the critical properties of fluids by means of light scattering, it has become clear that multiple scattering plays an important role. Only in experiments of limited accuracy, restricted to a qualitative study of the phenomena, can the complication of multiple scattering be overlooked. Even in cases where the fluid has been carefully constituted so as to minimize the intensity of the scattered light, such as the binary system 3-methyl pentane-nitroethane, it has proved to be essential to correct the data for double scattering. This is because the interesting critical effects under investigation are often rather subtle and depend upon high experimental accuracy. For example, the recent experimental determination by Chang *et al.*[1] of the critical exponent η required an accuracy of a small fraction of 1%. This was necessary because η itself is only of the order of 3%. Clearly, double scattering of the order of a few percent could completely mask the effect being studied. Fortunately Bray and Chang[2] found it possible to calculate the double-scattering intensity to sufficient accuracy for the geometry and parameters of the experiment. The present paper is an extension of the Bray-Chang work to dynamics, i.e., to the time dependence of the double-scattered light intensity.

One of the authors[3] has studied the effect of double scattering on linewidth measurements for the hydrodynamic regime, where the rate of diffusion has its normal quadratic dependence upon wave number. It was noted, as a consequence of the Pythagorean theorem, that the double-scattered light arriving in the backward direction has a linewidth independent of the two successive scatterings. For this special case, no double-scattering correction is required. But this result does not apply in the critical region, which is the case of interest in this paper. The calculations of Sorensen *et al.*,[4] are valid for the critical region but their spherical geometry, like that of Oxtoby and Gelbart,[5] unfortunately does not match the rectangular geometry of most experiments. The numerical work of Beysens and Zalcer[6] does not suffer from this latter shortcoming but their analytic description as a superposition of two discrete relaxation rates is not generally sufficiently accurate, as explained below in Sec. V.

Of special interest is the critical limit $k_0\xi \to \infty$, where k_0 is the wave number of the light in the scattering medium and ξ is the correlation length of the density or concentration fluctuations in a simple or binary fluid, respectively. In terms of the parameter $\alpha = (k_0\xi)^{-1}$ used by Bray and Chang, this corresponds to $\alpha \to 0$. (The α used by Puglielli and Ford[7] to describe this critical temperature dependence of the turbidity is twice the inverse square of the Bray-Chang α.) In this extreme critical, or "nonhydrodynamic," limit the wave-number dependence of the diffusion is expected to be nearly cubic. An additional consequence of the $\alpha = 0$ limit, as noted by Perl and Ferrell,[8] is a deviation from Lorentzian which is predicted in the shape of the frequency spectrum of the scattered light. Although small, this deviation is of considerable theoretical interest, as it offers a test of the theories of critical dynamics. Experimental precision has now attained a level where it will be possible to reveal such subtle small effects also in the dynamics. But just as

with the statics, it is essential to have a reliable treatment of the effect of double scattering on the frequency spectrum.

In order to focus this work we concentrate on $\alpha = 0$, with finite α studied in Appendix D. Although $\alpha = 0$ obviously eliminates any study of temperature dependence, there remains the interesting question of frequency dependence, as mentioned above. Results for the deviation of the double-scattered light from Lorentzian are presented below in Sec. V and are shown in Fig. 7. (Section V also exhibits in Fig. 5 the full distribution of relaxation rates.) It is, however, more convenient to work in time rather than in frequency space. This involves, of course, the Fourier transform, so that a Lorentzian spectrum transforms into an exponential function with a single decay rate. Let $I(\tau)$ represent the autocorrelation function of the electric field at the detector. We will, by way of abbreviation, refer to $I(\tau)$ as the "correlation function," or simply the "correlation." $I(0)$ represents the time-averaged light intensity. It is the double-scattering contribution to this quantity which was calculated by Bray and Chang.[2] Now in the absence of a deviation from a Lorentzian, the plot of $\ln I(\tau)$ vs τ will be a straight line with a negative slope equal to the relaxation rate. A deviation from Lorentzian leads, on the other hand, to a curved semilog plot. The various moments describing the deviation are characterized in Sec. II, while Sec. III is devoted to a computation of the second moment for both polarization possibilities. The higher moments are taken into account in Sec. IV by means of a "correction factor" on the second moment. The results are plotted in Fig. 4, where it will be noted that the correction factor does not differ from unity in the range of interest by more than 25%. Section V exhibits the double scattering as a continuum superposition of decay rates. The result is plotted in Fig. 5, while Fig. 7 shows the deviation from a Lorentzian spectrum that ensues from the distribution of rates. While both of these studies contribute to a deeper understanding of double scattering, they are not essential to the reader whose concern is primarily how to apply an appropriate double-scattering correction to photon-counting data. Furthermore, Sec. VI is restricted to $I(0)$ and has nothing to say about dynamics. Its purpose is to make contact with the work of Bray and Chang. By means of small-angle approximations, valid in the range $\alpha \ll 1$, where double scattering is most important, we obtain analytic expressions for the numerical results reported by Bray and Chang. The comparison is exhibited in Fig. 8.

From the above it will become apparent that the reader who is concerned only with the main effect of double scattering on dynamics may skip Secs. IV–VI and confine himself to Secs. I and II and III A. Section III B is devoted to calculating a relatively small correction which a reader, satisfied with logarithmic accuracy, could well skip. Similarly, Sec. III C deals with the less common case of parallel polarization (for which no single scattering occurs). Therefore after III A, the reader interested in the essentials could jump to Sec. VII, where we summarize how the results of III A are to be utilized. For the reader interested in further details we have provided the following four appendixes at the end of the paper: Appendix A—basic theory of double scattering including its spatial coherence; Appendix B—exact evaluation of the integrals encountered in Sec. III (to justify the much simpler treatment given there); Appendix C—extension of the correction factor of Sec. IV beyond the "practical" range treated there (this correction factor improves the simple theory of Sec. III, which, however, is adequate for many purposes); and Appendix D—temperature dependence of the double-scattering correction to the time-dependent correlation function.

B. Mathematical preliminaries

According to Ornstein-Zernike[9] theory the light scattering intensity per unit length and per unit solid angle is given by

$$I(\theta, \Phi) = B \sin^2\Phi / [\alpha^2 + (2 \sin\tfrac{1}{2}\theta)^2] \tag{1.1}$$

in the notation of Bray and Chang.[2] (B is a constant of the medium, θ the scattering angle, and Φ the angle between the initial direction of polarization and the direction of scattering.)

$$I(\theta, \Phi, t) = I(\theta, \Phi) e^{-\Gamma(\theta) t}, \tag{1.2}$$

where $\Gamma(\theta)$ is the relaxation rate for the specific fluctuation from which single scattering is taking place. As the angular dependence of $\Gamma(\theta)$ for $\alpha = 0$ is known from both theory and experiment to correspond to the cube of the momentum transfer, we can write

$$\Gamma(\theta) = \gamma_s \sin^3\tfrac{1}{2}\theta. \tag{1.3}$$

The proportionality constant is $\gamma_s = k_B T_c / 16\eta_s$ in Kawasaki's theory[10] or in an alternative form[11] presented by one of the authors. (η_s, T_c, and k_B are the viscosity, critical temperature, and Boltzmann's constant, respectively.) But, the actual value of γ_s not being relevant for our present purposes, it is left as a free parameter. Setting $\alpha = 0$ in Eq. (1.1) gives the simplified expression for the intensity for $\perp$ polarization,

$$I(\theta) = B(4 \sin^2\tfrac{1}{2}\theta)^{-1}. \tag{1.4}$$

As the deviations from Ornstein-Zernike theory are known to be small [of $O(\eta)$], Eq. (1.4) is adequate for computations of the double scattering

within an accuracy of 10%—which will be our goal in this paper. To calculate the double-scattering intensity, we specialize to the experimental arrangement shown in Fig. 1, which is identical to Fig. 1 of Bray and Chang.[2] The scattering volume is a cylinder of radius r_0 and height h. As the height will be taken to be very small, the simplified planar geometry as shown in Fig. 2 is valid in first approximation. Therefore, h appears as a simple multiplicative factor in the expression for the intensity of the double-scattered light. (The height dependence will be treated more accurately at the ends of Secs. III B and III C, as well as in Secs. VI and VII.) The effect of finite beam width is studied in Appendix A. For the rest of our work we assume that the light beam has negligible width and is incident along the negative y axis and is polarized in the z or x direction, in the $\perp$- and $\parallel$-polarization cases, respectively. The passage of the light for a typical double-scattering event is indicated by the double arrows in Fig. 2. The detector is in the positive x direction. Because of the right-angle geometry shown in Figs. 1 and 2 the single scattering must take place at 90°. Equations (1.4) and (1.3) therefore yield

$$I_s = I(\tfrac{1}{2}\pi) = \tfrac{1}{2}B, \tag{1.5}$$

$$\Gamma_s = \Gamma(\tfrac{1}{2}\pi) = \gamma_s/2\sqrt{2}. \tag{1.6}$$

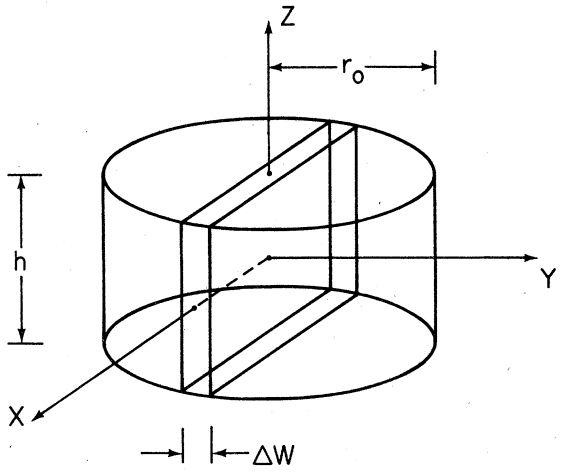

FIG. 1. Three-dimensional double-scattering geometry [after Bray and Chang (Ref. 2)]. The incident laser light comes from the source at $y=-\infty$ and after being scattered is incident upon the detector at $x=+\infty$. The width of the entrance window for the detector, Δw, is taken to be infinitely thin. The height and radius of the cylindrical sample of fluid are h and r_0, respectively. The single scattering takes place in the x-y plane, at $z=0$. The double scattering involves an initial scattering somewhere along the y axis, followed by a second scattering located somewhere in the rectangular slab shown centered about the x-z plane.

Equation (1.6) provides a convenient rate unit for our subsequent analysis. As can be seen from Fig. 2, the first scattering takes place at $(0,y)$ and the second at $(x,0)$. The scattering angles are θ and $\theta' = \frac{1}{2}\pi + \theta$. It is evident from the geometry that

$$x = -r\sin\theta, \quad y = -r\cos\theta, \tag{1.7}$$

where

$$x^2 + y^2 = r^2. \tag{1.8}$$

From Appendix A and Eq. (2.7) of Bray and Chang,[2] we have for the intensity $\epsilon_{in}^{\perp}$ of the double-scattered light in the $\perp$-polarization case

$$\epsilon_{in}^{\perp} = \int_{-r_0}^{r_0} dx \int_{-r_0}^{r_0} dy \int_{-h/2}^{h/2} dz \, \frac{I(\theta,\phi)I(\theta',\phi')}{r^2}. \tag{1.9}$$

From the approximations indicated above we find

$$\epsilon_{in}^{\perp} = \frac{hB^2}{16} \int_{-r_0}^{r_0} dx \int_{-r_0}^{r_0} dy \, \frac{1}{r^2} \frac{1}{\sin^2\frac{1}{2}\theta \sin^2(\frac{1}{4}\pi + \frac{1}{2}\theta)}. \tag{1.10}$$

The parallel-polarization case needs including in the integrand the polarization factor $\sin^2\theta\cos^2\theta$. A derivation of Eq. (1.10) from Maxwell's equations is presented in Appendix A. There, we also

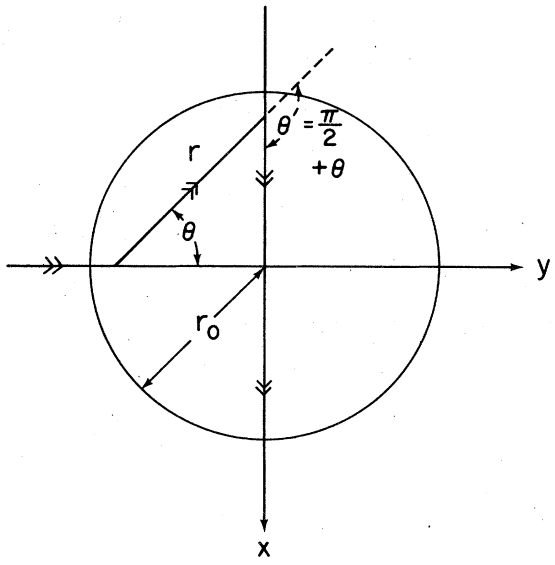

FIG. 2. Planar simplification of the three-dimensional scattering geometry of Fig. 1, adequate for scatterings in which the separation of the two scattering points, r, is much greater than h, the height shown in Fig. 1. The projection of the scattering in the x-y plane gives the projected angles of scattering at θ and $\theta' = \frac{1}{2}\pi + \theta$ for the first and second scatterings, respectively. The double arrows show the course of the doubly scattered light for a typical double-scattering event. As in Fig. 1, r_0 is the diameter of the scattering region, which in this case is a circle centered in the x-z plane.

determine the spatial coherence of the doubly scattered light and calculate the coherence areas A_s and A_D for single and double scattering, respectively. Although $A_D < A_s$, the difference is not great, provided that h is not much larger than the width of the beam in the z direction. This difference needs to be taken into account when A_P, the area of the photosensitive surface of the detector, is comparable to A_D. For the limiting case of $A_P \gg A_S > A_D$, the correction factor required by Eq. (1.10), in order that it be properly normalized relative to the single-scattering intensity, approaches A_D/A_s asymptotically. For a beam of rectangular cross section with overall vertical width $2w_B$, $A_D/A_s = 2w_B/h$. The corresponding factors for a beam of circular cross section and for a beam of Gaussian profile are given in Appendix A.

For the time-dependent case we must modify the above expression by including the decaying exponentials at each scattering point and thereby obtain

$$\epsilon_{1n}^{\perp}(t) = \frac{hB^2}{16}\int_{-r_0}^{r_0} dx \int_{-r_0}^{r_0} dy \frac{1}{r^2} \frac{\exp\{-[\Gamma(\theta)+\Gamma(\tfrac{1}{2}\pi+\theta)]t\}}{\sin^2\tfrac{1}{2}\theta \sin^2(\tfrac{1}{4}\pi+\tfrac{1}{2}\theta)}. \tag{1.11}$$

Finally, it is useful to introduce the turbidity τ_s, which is the total scattering intensity per unit length and is given by the integral of $I(\theta, \phi)$ over solid angle,[7]

$$\tau_s = \int d\Omega I(\theta,\phi) = \frac{1}{2}\pi B\left((1+\beta)\ln\frac{\sqrt{\beta}+1}{\sqrt{\beta}-1} - 2\sqrt{\beta}\right), \tag{1.12}$$

where

$$\beta = (1+\tfrac{1}{2}\alpha^2)^2. \tag{1.13}$$

For $\alpha \ll 1$, Eq. (1.12) simplifies to

$$\tau_s = \frac{1}{2}\pi B\left(2\ln\frac{4}{\alpha^2} - 2\right) = 2\pi B \ln\frac{2}{\alpha e^{1/2}}. \tag{1.14}$$

The total light "lost," or scattered out is

$$\epsilon_{\text{out}} = 4\pi r_0 B \ln(2/\alpha e^{1/2}) = 4\pi r_0 B S(\alpha), \tag{1.15}$$

where

$$S(\alpha) = \ln(2/\alpha e^{1/2}) \tag{1.16}$$

is a "scattering" function that expresses the critical dependence of ϵ_{out} on α. Equation (1.16) is valid only in the range $\alpha \ll 1$. Outside this range we have to return to Eqs. (1.12) and (1.13) for a more accurate expression for $S(\alpha)$. If necessary Eq. (1.14) can be used to determine experimentally the constant B, as τ_s can be measured at different values of α. We will assume that the turbidity is small, which implies that the constant B will be small as well. Also a small τ_s allows us to do our double-scattering integrals without worrying about the damping due to turbidity which would be a second-order effect. The smallness of B enables us to define the dimensionless small parameter ϵ by the relation

$$\epsilon = 4\pi r_0 B. \tag{1.17}$$

This will be useful in the subsequent sections. $\epsilon \ll 1$ is assumed throughout—otherwise triple scattering and even higher-order multiple scattering could not be neglected.

II. TIME-DEPENDENT CORRELATION FUNCTION

As we have seen above and in Appendix A the time decay of the amplitude of the scattered light can be decomposed into the two terms

$$I(t) = I_s e^{-\Gamma_s t} + \int dI_D e^{-\Gamma_D t} = I_s e^{-\tau}\left(1 + \frac{1}{I_s}\int dI_D e^{-(\Delta\Gamma/\Gamma_s)\tau}\right), \tag{2.1}$$

where the first term on the right-hand side represents the simple exponential decay of the singly scattered light, whereas the second term expressed by an integral is the decay of the double-scattered light according to various different relaxation times identified by the compound scattering rate Γ_D. We have introduced for convenience the dimensionless time measured in units of the single-scattering relaxation time by

$$\tau = \Gamma_s t, \tag{2.2}$$

and furthermore have introduced the difference between the compound and single relaxation rate by the relation

$$\Delta\Gamma = \Gamma_D - \Gamma_s. \tag{2.3}$$

The correlation is most conveniently studied in terms of its logarithm, which becomes

$$\ln I(t) = \ln I_s - \tau + \ln\left(1 + \frac{1}{I_s}\int dI_D e^{-\Delta\Gamma/\Gamma_s\tau}\right) = \ln I_s - \tau + \frac{1}{I_s}\int dI_D e^{-\Delta\Gamma/\Gamma_s\tau}. \tag{2.4}$$

Here we have approximated the logarithm linearly, which is permitted when the total intensity of the double-scattered light is small. To make further progress we expand the exponential function as

$$e^{-\Delta\Gamma/\Gamma_s\tau} = \sum_n \frac{(-1)^n}{n!}\left(\frac{\Delta\Gamma}{\Gamma_s}\right)^n \tau^n. \tag{2.5}$$

Thus we obtain the semilog plot for the correlation in the form of the Taylor series

$$\ln I(t)\ln I_s - \tau + \epsilon\sum_{n=0}^{\infty}(-1)^n C_n \tau^n, \tag{2.6}$$

where ϵ is defined by Eq. (1.17). The coefficients are

$$C_n=\frac{1}{\epsilon I_s n!}\int dI_D\left(\frac{\Delta\Gamma}{\Gamma_s}\right)^n . \tag{2.7}$$

The main effect comes from C_2, which is computed in Sec. III. This gives a concavity to the semilog plot. The effect of the terms $n\geq 3$ is evaluated in Sec. IV.

III. CONCAVE SEMILOG PLOT

A. Perpendicular polarization

In order to apply Eqs. (2.6) and (2.7) it is necessary to have a distribution for the differential double-scattered intensity dI_D. According to the discussion in Sec. I, the double scattering occurs at the two points in the sample identified by the Cartesian coordinates $(0,y)$ and $(x,0)$. As only one variable of each pair differs from zero, it is convenient to combine them together into a single pair and to make an effective polar-coordinate transformation to r and θ, according to Eqs. (1.7) and (1.8). We can immediately integrate out the radial coordinate. Thus we find for the total double-scattering intensity the following integral over angle:

$$\int dI_D^{\perp}=\frac{B^2h}{16}\int_{-r_0}^{r_0}dx\int_{-r_0}^{r_0}dy\,\frac{1}{r^2}\,\frac{1}{\sin^2\frac{1}{2}\theta\sin^2(\frac{1}{4}\pi+\frac{1}{2}\theta)}$$

$$=\frac{B^2h}{16}\ln\gamma\oint\frac{d\theta}{\sin^2\frac{1}{2}\theta\sin^2(\pi\frac{1}{4}+\frac{1}{2}\theta)} . \tag{3.1}$$

The integration over the radial coordinate extends out to a maximum value of $r_0\sec\theta$, or simply r_0, to logarithmic accuracy. Similarly the lower limit for the integration is $\frac{1}{2}h$, to logarithmic accuracy. This yields the factor $\ln\gamma=\ln(2r_0/h)$. An improvement of the calculation beyond logarithmic accuracy is presented in Sec. III B.

Identifying the integrand as the desired distribution of double scattering with respect to the angle θ, we have for the distribution function

$$\frac{dI_D^{\perp}}{d\theta}=\frac{hB^2}{16}\ln\gamma\,\frac{1}{\sin^2\frac{1}{2}\theta\sin^2(\frac{1}{4}\pi+\frac{1}{2}\theta)} . \tag{3.2}$$

According to Eq. (2.7) we must divide this distribution by the small quantity

$$\epsilon I_s=2\pi r_0B^2, \tag{3.3}$$

thus obtaining for the integrand that we require for application of Eq. (2.7) the ratio

$$\frac{1}{\epsilon I_s}\frac{dI_D^{\perp}}{d\theta}=\frac{\ln\gamma}{16\pi\gamma}\,\frac{1}{\sin^2\frac{1}{2}\theta\sin^2(\frac{1}{4}\pi+\frac{1}{2}\theta)} . \tag{3.4}$$

As noted above, the first qualitative difference produced by the double scattering occurs in the quadratic term of Eq. (2.6). Thus it is of considerable interest to obtain the coefficient of this quadratic term which, according to Eq. (2.7) can be written

$$C_2^{\perp}=\frac{\ln\gamma}{2!\gamma}\oint f_{\perp}(\theta)\,d\theta , \tag{3.5}$$

where the integrand is defined as the function of angle

$$f_{\perp}(\theta)=\frac{1}{16\pi}\,\frac{(\Delta\Gamma/\Gamma_s)^2}{\sin^2\frac{1}{2}\theta\sin^2(\frac{1}{4}\pi+\frac{1}{2}\theta)} . \tag{3.6}$$

In order to carry out the integration indicated in Eq. (3.5) we require a specific expression for the numerator of Eq. (3.6). It is useful to study this quantity in the vicinity of $\theta=0$ where it serves to cancel the singularity occurring in the denominator. (Similar cancellation occurs in the vicinity of $\theta=-\frac{1}{2}\pi$.) Two-step application of the relaxation rate for single scattering yields

$$\Gamma_D=\Gamma_s(\theta)+\Gamma_s(\theta+\tfrac{1}{2}\pi). \tag{3.7}$$

Substitution from Eqs. (1.3) and (2.3) gives

$$\Delta\Gamma(\theta)=\gamma_s(\left|\sin^3\tfrac{1}{2}\theta\right|+\left|\sin^3(\tfrac{1}{4}\pi+\tfrac{1}{2}\theta)\right|-1/2\sqrt{2}). \tag{3.8}$$

The derivative of this expression evaluated at the origin is

$$\left.\frac{d}{d\theta}\Delta\Gamma(\theta)\right|_{\theta=0}=\tfrac{3}{2}\gamma_s\sin^2\tfrac{1}{4}\pi\cos\tfrac{1}{4}\pi$$

$$=\tfrac{3}{2}\gamma_s\sin^3\tfrac{1}{4}\pi$$

$$=\tfrac{3}{2}\Gamma_s. \tag{3.9}$$

Therefore for small angles,

$$\Delta\Gamma(\theta)/\Gamma_s\cong\tfrac{3}{2}\theta \tag{3.10}$$

so that the zero in the numerator does indeed cancel the zero in the denominator of Eq. (3.6). This gives for the value of the function at the origin,

$$f_{\perp}(0)=\frac{9}{16\pi}\,\frac{1}{\sin^2\frac{1}{4}\pi}=\frac{9}{8\pi} . \tag{3.11}$$

$f(\theta)$ is roughly constant, as seen in Fig. 3. Therefore, the integral in Eq. (3.5) can be approximated satisfactorily by setting $f(\theta)$ everywhere equal to its value at $\theta=0$. Factoring $f(0)$ out of the integration gives

$$\oint f_{\perp}(\theta)\,d\theta\simeq f_{\perp}(0)\oint d\theta=2f_{\perp}(0)=\frac{9}{4} . \tag{3.12}$$

[An exact evaluation of this integral in Appendix B shows Eq. (3.12) to be sufficiently accurate, being an overestimate by only 5%.] Substituting this result into Eq. (3.5) gives us finally the desired expression solely in terms of the basic experimental parameters of the problem, ϵ and γ as

$$\epsilon C_2^{\perp}\tau^2=\tfrac{9}{8}(\ln\gamma+c)\tau^2/\gamma. \tag{3.13}$$

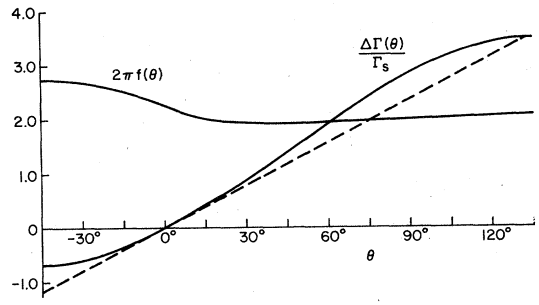

FIG. 3. Functions involved in the curvature calculation vs θ, the angle of the first scattering. Γ_s is the relaxation rate for single scattering while $\Delta\Gamma(\theta)$ is the difference of the relaxation rates for double and single scattering. The dashed line shows the "linear approximation" fit, while the remaining curve shows the function $2\pi f(\theta)$ which appears in the integrand for the curvature. The linear approximation replaces $f(\theta)$ by $f(0)$ (with a resulting error of 5%).

In Eq. (3.13) we have introduced a correction c to $\ln\gamma$, which we now proceed to calculate. In Sec. III B we find $c_u + c_l = 0.13$, by computing separately $c_{u,l}$, the upper- and lower-cutoff contributions. This is a small effect even for modest values of $\ln\gamma$. Therefore the reader who is satisfied with logarithmic accuracy could skip the entire Sec. III B.

B. Correction to the logarithm

The three-dimensional integration in Eq. (3.1) was separated into an angular integration and an integration over the radial and height variables, r and z, respectively. The planar geometry breaks down when r, the projection onto the x-y plane of the separation of the points of scattering, becomes smaller than z, the vertical separation of the two points. We therefore cut off the radial integration at the lower limit $r = |z|$, obtaining the result

$$\int_{-h/2}^{h/2} dz \int_{|z|}^{r_0} \frac{dr}{r} = 2\int_0^{h/2} dz \ln\frac{r_0}{z} = h(\ln 2r_0/h + 1) = h(\ln\gamma + 1), \tag{3.14}$$

which contributes 1 to c_l.

Immediately following Eq. (3.1) we noted an improvement in the upper limit. The latter should occur at $r = r_0 \sec\theta$ rather than simply r_0. Therefore the integrand includes the additional term

$$\ln\sec\theta = \sec\theta - 1 - \tfrac{1}{2}(\sec\theta - 1)^2 + \cdots = \tfrac{1}{2}(\sec\theta - 1) + \tfrac{1}{2}(1 - \cos\theta) + \cdots . \tag{3.15}$$

The last way of writing the expansion is convenient for calculating angle averages and agrees with the Taylor series expansion to second order. The required angular averages need only be taken over one octant, in the interval $0 < \theta < \frac{1}{4}\pi$ and yield the numerical results

$$\langle(1 - \cos\theta)\rangle = 0.099 , \tag{3.16}$$

$$\langle(\sec\theta - 1)\rangle = 0.121. \tag{3.17}$$

The correction to the upper cutoff is therefore

$$\langle\ln\sec\theta\rangle = c_u = 0.110. \tag{3.18}$$

A natural cutoff at the lower end of the radial integration occurs as soon as we take into account properly the fact that the distance between the two scattering points is given not simply by the projection in the plane but instead by the total distance

$$R = (x^2 + y^2 + z^2)^{1/2} = (r^2 + z^2)^{1/2}. \tag{3.19}$$

Introducing this change gives the radial integral

$$\int_0^{r_0} \frac{r\,dr}{R^2} = \frac{1}{2}\int_0^{r_0} \frac{d(r^2)}{r^2 + z^2} = \frac{1}{2}\ln\frac{z^2 + r_0^2}{z^2} \simeq \ln\left(r_0/|z|\right). \tag{3.20}$$

The introduction of the lower cutoff is thus put on a firmer basis, justifying the appearance in Eq. (3.14) of the quantity $\ln r_0/z$. If this modification were the only physical effect occurring in the three-dimensional geometry, Eq. (3.14) and (3.18) would be the final answer and we would conclude that $c = c_l + c_u = 1.11$.

There are, however, other complications which enter into the three-dimensional double-scattering situation, such as polarization. When the scattering takes place out of the x-y plane, the polarization vector for the intermediate radiation propagating between the two scattering points is tilted away from its initial direction (along the z axis) and becomes

$$\xi_I = -\frac{xz}{rR}\vec{\mathrm{i}} + \frac{zy}{rR}\vec{\mathrm{j}} + \frac{r}{R}\vec{\mathrm{k}} . \tag{3.21}$$

The unit vectors $\vec{\mathrm{i}}$, $\vec{\mathrm{j}}$, and $\vec{\mathrm{k}}$ are directed along the three Cartesian axes x, y, and z, respectively. The first scattering is weakened by the square of the cosine of the angle between the initial and intermediate polarization vectors, namely, r^2/R^2. The polarization factor entering into the second scattering is more complicated. Including both factors, we find

$$P(r^2/z^2, \theta) = (r^2/R^2)(1 - x^2z^2/r^2R^2) = r^2/R^2 - x^2z^2/R^4 . \tag{3.22}$$

Replacing x^2 by its angular averaged value, $1/2r^2$, gives

$$\langle P\rangle_\theta = r^2/R^2 - \frac{1}{2}z^2r^2/R^4 \tag{3.23}$$

We now turn to the modification of Eq.(3.6) required by the three-dimensional geometry. If θ and θ' are the first and second scattering angles in this three-dimensional double-scattering situation, then the function corresponding to Eq. (3.6) requires, over and above its dependence on θ, an additional dependence on the ratio r^2/z^2 as defined by

$$f\left(\theta;\frac{r^2}{z^2}\right)=\frac{(|\sin^3\tfrac{1}{2}\Theta|+|\sin^3\tfrac{1}{2}\Theta'|-1/2\sqrt{2})^2}{2\pi\sin^2\tfrac{1}{2}\Theta\sin^2\tfrac{1}{2}\Theta'}. \tag{3.24}$$

The dependence of this function on Θ and Θ' makes it inconvenient to use. Fortunately the function has some simplifying features. First of all, for $r^2\gg z^2$, we recover Eq. (3.6). We further recall that $f(\theta)$ is practically constant, and to a good approximation can be replaced by its $\theta=0$ value, $f(0)=9/8\pi$. In the other extreme, $r^2\ll z^2$, both scatterings take place on the z axis and both scattering angles are equal to $\frac{1}{2}\pi$. Equation (3.24) then reduces to

$$f(\theta;0)=1/4\pi=\tfrac{2}{9}f(0), \tag{3.25}$$

a factor $\frac{2}{9}$ smaller than its other limiting value. Between these limiting cases, it is reasonable to do angle averaging, leaving us with a function of only the one variable r^2/z^2. We, in fact, compute the θ average only to $O(r^2/z^2)$, thereby determining the initial departure of Eq. (3.24) from Eq. (3.25). This leads us to the interpolation formula

$$\left\langle f\left(\theta;\frac{r^2}{z^2}\right)\right\rangle_\theta=\frac{r^2/z^2+\frac{7}{9}}{r^2/z^2+\frac{7}{2}}f(0). \tag{3.26}$$

Having approximated all of the correction factors in the integrand of Eq. (3.1) by their angular averages, we can now carry out the integration over the variable $u=r^2/z^2$. It is convenient to compare this integration with the "reference" integration of Eq. (3.20). This gives for c_l, the additional correction to the logarithm coming from the lower cutoff, the difference

$$\begin{aligned}\frac{1}{2}\int_0^{r_0^2/z^2}\frac{du}{u+1}\langle P\rangle_\theta\langle f\rangle_\theta-\frac{1}{2}\int_0^{r_0^2/z^2}\frac{du}{u+1}f(0)&\\ =\frac{f(0)}{2}\int_0^\infty\frac{du}{u+1}\left(\langle P\rangle_\theta\frac{\langle f\rangle_\theta}{f(0)}-1\right)&\\ =f(0)c_l.&\end{aligned} \tag{3.27}$$

Because the difference integrand gives a convergent integral, it is permitted to set the upper limit equal to ∞. Elementary integration then yields

$$\begin{aligned}c_l=\frac{1}{2}\int_0^\infty\frac{du}{1+u}\left[\left(\frac{u}{1+u}-\frac{1}{2}\frac{u}{(1+u)^2}\frac{u+\frac{7}{9}}{u+\frac{7}{2}}-1\right)\right]&\\ =-0.98.&\end{aligned} \tag{3.28}$$

The total correction to the logarithm is found by collecting the contributions from Eqs. (3.14), (3.18), and (3.28),

$$c=1+c_u+c_l=0.13, \tag{3.29}$$

a result which has been quoted following Eq. (3.13).

C. Parallel polarization

As explained above, the differential cross section for parallel polarization requires the inclusion of the factor $\sin^2\theta\cos^2\theta$ in the numerator of Eq. (3.2), and consequently also in the numerator of Eq. (3.6). We continue to approximate the angular dependence of the double-scattering width by Eq. (3.10), our so-called "linear approximation," which gives for the modified form of Eq. (3.6),

$$f_{\parallel}(\theta)=\frac{9}{64\pi}\frac{\theta^2\sin^2\theta\cos^2\theta}{\sin^2\tfrac{1}{2}\theta\sin^2(\tfrac{1}{4}\pi+\tfrac{1}{2}\theta)}. \tag{3.30}$$

The corresponding curvature correction is again to be obtained from Eq. (3.5), but with $f_{\parallel}(\theta)$ in place of $f_\perp(\theta)$. If, as before, we approximate the denominator of Eq. (3.14), by $\frac{1}{8}\theta^2$, then the only angular dependence occurring in $f_{\parallel}(\theta)$ is that introduced by the polarization factor. It is convenient to rewrite this in the form

$$\begin{aligned}\sin^2\theta\cos^2\theta&=\tfrac{1}{4}\sin^2 2\theta\\ &=\tfrac{1}{8}-\tfrac{1}{8}\cos 4\theta.\end{aligned} \tag{3.31}$$

Clearly, the last term vanishes in the integration over angle, leaving the result

$$\oint f_{\parallel}(\theta)\,d\theta=\tfrac{1}{8}\tfrac{9}{4}=\tfrac{9}{32}. \tag{3.32}$$

Thus, with the above approximations, parallel polarization reduces the expected curvature by a factor of $\frac{1}{8}$. The leading nonlinear term is consequently

$$\epsilon C_2^{\parallel}\tau^2=\tfrac{9}{64}\epsilon(\ln\gamma+c')\tau^2/\gamma, \tag{3.33}$$

where $c'=0.67$ is the correction to the logarithm for parallel polarization. The evaluation is carried out as above in Sec. III B for perpendicular polarization. The contributions at the upper and lower cutoffs are $c_u'=0.18$ and $c_l'=-0.51$, respectively, giving $c'=1+c_u'+c_l'=0.67$.

Equation (3.17) solves the problem which we set for ourselves in this subsection. It is, however, instructive to apply an alternative approximation which is based on the factorization

$$\begin{aligned}\sin^2\theta\cos^2\theta&=(1-\cos^2\theta)(1-\sin^2\theta)\\ &=(1-\cos\theta)(1+\cos\theta)\\ &\quad\times(1-\sin\theta)(1+\sin\theta).\end{aligned} \tag{3.34}$$

The denominator of Eq. (3.14), instead of being written as a quadratic expression can be put into the form

$$\sin^2\tfrac{1}{2}\theta \sin^2(\tfrac{1}{2}\theta+\tfrac{1}{4}\pi)=\tfrac{1}{4}(1-\cos\theta)(1+\sin\theta). \tag{3.35}$$

Thus, the denominator conveniently cancels with some of the factors of the numerator, leaving

$$\frac{\sin^2\theta\cos^2\theta}{\sin^2\tfrac{1}{2}\theta\sin^2(\tfrac{1}{4}\pi+\tfrac{1}{2}\theta)}=4(1+\cos\theta)(1-\sin\theta). \tag{3.36}$$

Consequently, we are left with the greatly simplified expression

$$f_{\parallel}(\theta)=(9/16\pi)\theta^2(1+\cos\theta)(1-\sin\theta). \tag{3.37}$$

It is more important to note that this expression can be expected to be a satisfactory approximation to $f_{\parallel}(\theta)$ only over one-half of the total range of variation of θ, namely, $-\frac{1}{4}\pi \leq \theta \leq \frac{3}{4}\pi$ (see Sec. IV A). Therefore, in evaluating the integral over the entire interval of 2π, we must include a factor of 2, so that elementary integration gives

$$2\int_{-\pi/4}^{3\pi/4} f_{\parallel}(\theta)\,d\theta=\frac{9}{32}\left(1+\frac{7\pi^2}{12}-4\sqrt{2}\right)$$

$$=1.10\times\tfrac{9}{32}\,. \tag{3.38}$$

This result differs only by 10% from that of Eq. (3.32) and indicates that, to this accuracy, the approximations being used are satisfactory for our purpose.

IV. FURTHER NONLINEARITIES

A. Perpendicular polarization

We have seen in Sec. II that the double scattering produces a deviation from linear behavior of the semilog plot of the correlation versus time, as expressed by Eq. (2.4). It is convenient to separate out the last term of Eq. (2.4) into constant and linear contributions. In other words, we consider the first two terms of the expansion of the exponential function in the integrand on a separate footing and define the remaining nonlinear contribution to the logarithm of the correlation by

$$(\ln I)_{\mathrm{nl}}=\frac{1}{I_s}\int dI_D\left(e^{-\Delta\Gamma/\Gamma_s\tau}-1+\frac{\Delta\Gamma}{\Gamma_s}\tau\right). \tag{4.1}$$

This puts Eq. (2.4) into the form

$$\ln I(t)=\ln I_s+\frac{1}{I_s}\int dI_D$$

$$-\tau\left(1+\frac{1}{I_s}\int dI_D\frac{\Delta\Gamma}{\Gamma_s}\right)+(\ln I)_{\mathrm{nl}}. \tag{4.2}$$

Thus we see that there is a double-scattering correction to the zero-time intercept of the semilog plot of the correlation. More important, there is also a double-scattering contribution to its slope, as expressed by the second term of the right-hand side of Eq. (4.2). We will return to this point in Sec. VII where we find that this term turns out to be negligibly small. Our interest in this section is to study further details of the last term of Eq. (4.2).

For this it is convenient to introduce, for the moment, a modified time variable

$$\bar{\tau}=\tfrac{3}{2}\tau. \tag{4.3}$$

As in Sec. III, we again approximate the denominator of the integrand by an inverse square dependence on θ:

$$\frac{1}{I_s}\frac{dI_D^{\perp}}{d\theta}\approx\epsilon\,\frac{\ln\gamma}{\pi\gamma}\frac{1}{\theta^2}\,. \tag{4.4}$$

As explained in Sec. III, this treatment is most accurate in the vicinity of the origin. It becomes inadequate as the second singularity of the right-hand side of Eq. (3.4) is approached for $\theta=-\frac{1}{2}\pi$. In the vicinity of this second singularity the zero of $\Delta\Gamma/\Gamma_s$ causes the same cancellation to occur that takes place at the origin. Thus, the behavior of the integrand in the right-hand side of Eq. (4.1) is duplicated in the vicinity of $-\frac{1}{2}\pi$. Because of this duplication, it is sufficient to carry out the θ integration only over an interval of π rather than 2π. The lower end of the range of integration is placed halfway between the two singularities, so that the range of integration is $-\frac{1}{4}\pi \leq \theta \leq \frac{3}{4}\pi$. Including the required factor of 2, we find

$$(\ln I)_{\mathrm{NL}}^{\perp}=\epsilon\,\frac{\ln\gamma}{\pi\gamma}\int_{-\pi/4}^{3\pi/4}\frac{d\theta}{\theta^2}(e^{-\bar{\tau}\theta}-1+\bar{\tau}\theta)$$

$$=\frac{\bar{\tau}\epsilon\ln\gamma}{\pi\gamma}\int_{-\pi\bar{\tau}/4}^{3\pi\bar{\tau}/4}\frac{dx}{x^2}(e^{-x}-1+x). \tag{4.5}$$

The indefinite integral encountered in Eq. (4.5) can be simplified by an integration by parts, giving

$$\int\frac{dx}{x^2}(e^{-x}-1+x)=-\frac{1}{x}(e^{-x}-1)-1$$

$$-\int\frac{dx}{x}(e^{-x}-1). \tag{4.6}$$

The last term in Eq. (4.6) can be studied by means of a Taylor series expansion which then permits an identification with the integral exponential function. This identification for positive values of x reads

$$\int\frac{dx}{x}(e^{-x}-1)=\sum_{k=1}^{\infty}\frac{(-1)^k}{kk!}x^k$$

$$=\mathrm{Ei}(-x)-\ln x-C, \tag{4.7}$$

where $C=0.577$ is Euler's constant. For negative values of x the definition of the integral exponen-

tial function differs somewhat, and has to be written

$$\int \frac{dx}{x}(e^{-x}-1)=\sum_{k=1}^{\infty}\frac{1}{kk!}|x|^k$$

$$=\overline{\mathrm{Ei}}(|x|)-\ln|x|-C. \tag{4.8}$$

Putting the integration limits from Eq. (4.5) into the indefinite integrals of Eqs. (4.7) and (4.8) gives us finally the following explicit expression for the logarithm of the correlation as a function of $\bar{\tau}$:

$$\begin{aligned}(\ln I)_{\mathrm{NL}} &=\epsilon(\ln\gamma/\pi\gamma)\{(4/3\pi)(1-e^{-3\pi\bar{\tau}/4})\\ &\quad -4/\pi(e^{\pi\bar{\tau}/4}-1)+\bar{\tau}\ln 3\\ &\quad -\bar{\tau}[\mathrm{Ei}(-\tfrac{3}{4}\pi\bar{\tau})-\overline{\mathrm{Ei}}(\tfrac{1}{4}\pi\bar{\tau})]\}.\end{aligned} \tag{4.9}$$

The Taylor series expansion for Eq. (4.9), apart from the constant and linear terms, is equivalent to that indicated already in Eq. (2.6). The leading term, as expected, is quadratic in the time variable and corresponds exactly to the curvature calculation of Sec. III. Thus it is possible to define a correction factor $F(\tau)$, which expresses the deviation of the function of Eq. (4.9) from a simple quadratic dependence on the time variable, as

$$(\ln I)^{\perp}_{\mathrm{NL}}=\tfrac{9}{8}\epsilon(\ln\gamma/\gamma)\tau^2F_{\perp}(\tau). \tag{4.10}$$

Reinstating the original time variable $\tau=\frac{2}{3}\bar{\tau}$ and substituting Eq. (4.9) into Eq. (4.10) gives

$$F_{\perp}(\tau)=\frac{8}{9\pi\tau^2}\left\{\frac{4}{3\pi}(1-e^{-9\pi\tau/8})+\frac{3}{2}\tau\ln 3-\frac{4}{\pi}(e^{3\pi\tau/8}-1)\right.$$
$$\left.-\frac{3\tau}{2}\left[\mathrm{Ei}\left(-\frac{9\pi\tau}{8}\right)-\overline{\mathrm{Ei}}\left(\frac{3\pi\tau}{8}\right)\right]\right\}. \tag{4.11}$$

This correction factor is plotted in Fig. 4 for the interval $0\leq\tau\leq 2.5$. For small values of τ, it first drops linearly, then exhibits a minimum at $\tau=1.7$, followed by a subsequent slow rise.

A tolerably good fit in the interval $0\leq\tau\leq 2.5$ is provided by the parabola

$$F_{\perp}=1-0.282\tau+0.083\tau^2. \tag{4.12}$$

This fit should not be confused with the Taylor series expansion, which has the coefficients -0.393 and 0.219, and which exhibits a less-deep minimum at a smaller value of τ. The discrepancy is attributable to the higher-order terms, which Eq. (4.12) effectively takes into account in an approximate way. For larger values of τ, Eq. (4.11) will become inaccurate and will overestimate the correction factor, because of the approximations used. Because of counting rate limitations, the interval $0\leq\tau\leq 2.5$ can be expected to be adequate for most practical applications. Some further aspects of the large-τ behavior of $F(\tau)$ are, however, studied in Appendix C.

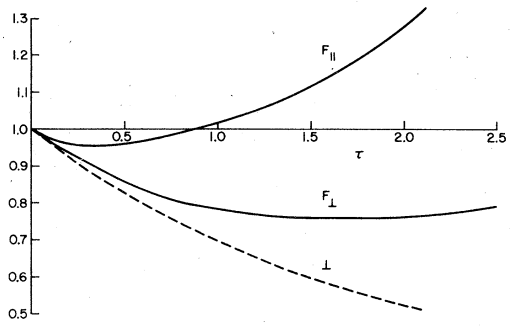

FIG. 4. Correction factors for perpendicular (⊥) and parallel (∥) polarization vs delay time τ (measured in units of the single-scattering relaxation time). The dashed line illustrates the result of imposing a two-δ-function fit on the continuum distribution of relaxation rates.

B. Parallel polarization

The calculation of the full time dependence of the nonlinear part of the logarithm of the correlation for parallel polarization is again based on Eq. (4.1). The calculation goes through in a way similar to that shown above in Sec. IV A. for the perpendicular-polarization case. However, in order to bring out the basic simplicity of the calculation, we present it now in a somewhat different form. We note, when we use the linear approximation, the integrand of Eq. (4.1) can be written in the form

$$e^{-\Delta\Gamma/\Gamma_s\tau}-1+\Delta\Gamma/\Gamma_s\tau=e^{-\bar{\tau}\theta}-1+\bar{\tau}\theta$$
$$=(1/2!)\bar{\tau}^2\theta^2+\cdots. \tag{4.13}$$

Here we have made the Taylor series expansion and have exhibited only the leading term. It is only this term which is important at small values of time and which, therefore, leads to the so-called curvature correction which was calculated in Sec. III C. Clearly, in order to obtain the correct time dependence for larger values of τ, we need to replace in the curvature calculation the leading term in the expansion of Eq. (4.13) by the full function which appears as the left-hand side of this equation. Thus, we define a "corrected" integrand for the calculation for the integral which appears in Eq. (3.38) by including in the integrand the ratio of the full function to its leading term. Substituting from Eq. (3.37), this gives us for the integrand the corrected function

$$\bar{f}_{\parallel}(\theta,\bar{\tau}) = (2/\bar{\tau}^2\theta^2)(e^{-\bar{\tau}\theta} - 1 + \bar{\tau}\theta) f_{\parallel}(\theta)$$

$$= \frac{9}{8\pi\bar{\tau}^2}(1+\cos\theta)(1-\sin\theta)(e^{-\bar{\tau}\theta} - 1 + \bar{\tau}\theta). \tag{4.14}$$

The integral of Eq. (3.38) is now the time-dependent function

$$J(\tau) = \int_{-\pi/4}^{3\pi/4} d\theta \bar{f}_{\parallel}(\theta,\tau). \tag{4.15}$$

For $\bar{\tau} \ll 1$ we must recover the curvature factor. Therefore, according to the definition of the correction factor as defined in Sec. IV A [see, for example, Eq. (4.10)], the correction factor for parallel polarization must be expressed by the ratio of Eq. (4.15) for finite times compared to its value at $\tau = 0$. In other words,

$$F_{\parallel}(\tau) = J(\bar{\tau})/J(0) = J(3/2\tau)/J(0). \tag{4.16}$$

Integration of Eq. (4.15) yields the explicit expression

$$J(\bar{\tau}) = \frac{9}{8\pi\bar{\tau}^2}\left\{ e^{\pi\bar{\tau}/4}\left(\frac{1}{\bar{\tau}} + \frac{\bar{\tau}}{2(4+\bar{\tau}^2)} + \frac{\sqrt{2}\,\bar{\tau}}{1+\bar{\tau}^2}\right) - e^{-3\pi\bar{\tau}/4}\left(\frac{1}{\bar{\tau}} + \frac{\bar{\tau}}{2(4+\bar{\tau}^2)} - \frac{\sqrt{2}\,\bar{\tau}}{1+\bar{\tau}^2}\right) - \pi - \left[2\sqrt{2} - 4\left(\frac{\pi}{4}\right)^2\right]\bar{\tau}\right\}. \tag{4.17}$$

Substituting Eq. (4.17) into Eq. (4.16) and plotting versus τ gives us the upper curve in Fig. 4 (labeled by "||"). It will be seen that this correction factor does not dip as much as $F_{\perp}$ and becomes greater than unity for $\tau > 0.9$.

V. DISTRIBUTION OF RELAXATION RATES

In the above work we have studied the distribution of the various contributions to the double scattering as a function of the first angle of scattering θ. It is useful, however, to reformulate this distribution and to study it as a function of the total relaxation rate for the double scattering. This is possible because, for every value of θ, there corresponds a particular value of the net relaxation rate resulting from the two scatterings that take place. It is convenient to introduce the variable ω to describe the deviation of the double-scattering relaxation rate from the single-scattering relaxation rate. By substitution from Eq. (3.8), we obtain, consequently,

$$\omega = \Delta\Gamma(\theta)/\Gamma_s = 2\sqrt{2}\left[\left|\sin^3\tfrac{1}{2}\theta\right| + \sin^3(\tfrac{1}{4}\pi + \tfrac{1}{2}\theta) - 1/2\sqrt{2}\right]. \tag{5.1}$$

According to Eq. (5.1) ω ranges between $\omega_1 = \omega(-\frac{1}{4}\pi) = -0.69$ and $\omega_2 = \omega\frac{3}{4}\pi) = 3.48$. In order to study the distribution of the double-scattering intensity as a function of ω instead of θ, we need

$$d\theta = \left(\frac{d\omega}{d\theta}\right)^{-1} d\omega. \tag{5.2}$$

The "Jacobian" of this transformation is consequently obtained by substitution from Eq. (5.1) and found to be

$$\omega'(\theta) = \frac{d\omega}{d\theta} = 3\sqrt{2}\left[\sin^2\tfrac{1}{2}\theta\cos\tfrac{1}{2}\theta\,\mathrm{sgn}\,\theta + \sin^2(\tfrac{1}{2}\theta + \tfrac{1}{4}\pi)\cos(\tfrac{1}{2}\theta + \tfrac{1}{4}\pi)\right]. \tag{5.3}$$

The differential double-scattering intensity is given in Eq. (3.4). Substituting from Eq. (3.4) and using Eqs. (5.2) and (5.3) in order to eliminate θ and replace it by ω leads us to define a distribution function $P(\omega)$ according to

$$\frac{1}{\epsilon I_s} dI_D = 2\,\frac{\ln\gamma}{16\pi\gamma}\,\frac{d\theta}{\sin^2\tfrac{1}{2}\theta\sin^2(\tfrac{1}{4}\pi + \tfrac{1}{2}\theta)} \cdot$$

$$= [(\ln\gamma)/\gamma] P(\omega)\, d\omega. \tag{5.4}$$

A factor of 2 has been included to take account of the twofold duplication of the interval $\omega_1 \le \omega \le \omega_2$ which occurs when θ runs through a full interval of 2π. Thus it follows that

$$P(\omega) = \frac{1}{8\pi}\,\frac{1}{\omega'(\theta)}\,\frac{1}{\sin^2\theta\sin^2(\tfrac{1}{4}\pi + \tfrac{1}{2}\theta)} \cdot \tag{5.5}$$

In the right-hand side of Eq. (5.5) it is understood that the variable θ is determined from Eq. (5.1) by inverting the functional relationship which is defined there. It is useful to study Eq. (5.5) in the vicinity of $\omega = 0$. For this we need

$$\omega'(0) = \tfrac{3}{2} \tag{5.6}$$

and

$$\omega \simeq \tfrac{3}{2}\theta\,. \tag{5.7}$$

Equations (5.6) and (5.7) are equivalent to Eqs. (3.9) and (3.10), respectively. With these linear approximations, valid for $|\omega| \ll 1$, we obtain by substitution into Eq. (5.5)

$$P(\omega) \approx \frac{2}{3\pi}\,\frac{1}{\theta^2} \approx \frac{3}{2\pi}\,\frac{1}{\omega^2} \cdot \tag{5.8}$$

This singularity dominates the behavior of the distribution of double-scattering relaxation rates and is, in fact, a rather good approximation over most of the range of variation of ω. For example, at $\theta = \frac{1}{2}\pi$ the derivative is

$$\omega'(\tfrac{1}{2}\pi) = \tfrac{3}{2}, \tag{5.9}$$

exactly the same value as at the origin [see Eq. (5.6)]. The value of ω at this angle is

$$\omega(\tfrac{3}{2}\pi) = 2\sqrt{2}\,, \tag{5.10}$$

or 2.828. Equation (5.7) gives for the linear approximation $\omega = \frac{3}{4}\pi = 2.36$, or about 20% less than the exact value. The exact value for the distribution function at this value of ω is, according to Eq. (5.5)

$$P(2\sqrt{2}) = 1/6\pi \ . \tag{5.11}$$

This can be compared with the approximate value of Eq. (5.8), which gives $3/16\pi$, or about 12% greater than the exact value.

Equation (5.8) for the distribution of double-scattering intensity versus ω, as we have seen above, is a satisfactory approximation over a wide range of ω. However, it is clear that the approximation fails at the end points ω_1 and ω_2. At these end points the function $\omega(\theta)$ exhibits extremum values and therefore completely different approximations are necessary to bring out the salient features of the distribution in the vicinity of these end points. It is sufficient for our purposes to use a quadratic approximation of the form

$$\omega(\theta) = \omega_1 + \tfrac{1}{2}(\theta + \tfrac{1}{4}\pi)^2 \omega_1'' \tag{5.12}$$

and

$$\omega(\theta) = \omega_2 + \tfrac{1}{2}(\theta - \tfrac{3}{4}\pi)^2 \omega_2'' = \omega_2 - \tfrac{1}{2}(\tfrac{3}{4}\pi - \theta)^2 \left|\omega_2''\right| . \tag{5.13}$$

The second derivatives are denoted by double primes and we have taken the absolute value of the second derivative at the upper limit because the curvature is negative at that point. We note that, because of the quadratic approximation in Eqs. (5.12) and (5.13), the denominator of Eq. (5.5) has a square-root singularity of the form

$$\omega'(\theta) = (\theta + \tfrac{1}{4}\pi)\omega_1'' = [2\omega_1''(\omega - \omega_1)]^{1/2} \tag{5.14}$$

and

$$\omega'(\theta) = (\tfrac{3}{4}\pi - \theta)\left|\omega_2''\right| = [2\left|\omega_2''\right|(\omega_2 - \omega)]^{1/2} . \tag{5.15}$$

The remaining factors in the denominator are well behaved at the end points and are

$$\sin^4 \tfrac{1}{8}\pi = \tfrac{1}{4}(1 - \cos\tfrac{1}{4}\pi)^2 = \tfrac{1}{4}(\tfrac{3}{2} - \sqrt{2}) = 0.0214 \tag{5.16}$$

and

$$\sin^4 \tfrac{3}{8}\pi = \tfrac{1}{4}(1 - \cos\tfrac{3}{4}\pi)^2 = \tfrac{1}{4}(\tfrac{3}{2} + \sqrt{2}) = 0.729 . \tag{5.17}$$

It is convenient to represent the above results in the form

$$P(\omega) = b_1/(\omega - \omega_1)^{1/2} \tag{5.18}$$

and

$$P(\omega) = b_2/(\omega_2 - \omega)^{1/2} \tag{5.19}$$

at the lower and upper end points, respectively. Numerical values for ω_1 and ω_2 have been given immediately following Eq. (5.1). The coefficients are $b_1 = 0.825$ and $b_2 = 0.031$. Equations (5.18) and (5.19) represent the singular behavior of the distribution function over certain small intervals, $\Delta\omega_1$ and $\Delta\omega_2$, respectively. We estimate the size of $\Delta\omega_{1,2}$ by matching Eqs. (5.18) and (5.19) to Eq. (5.8). Using for the moment the end-point values $\omega_{1,2}$ for approximating Eq. (5.8), we find

$$\Delta\omega_{1,2} = (\tfrac{4}{9}\pi^2) b_{1,2}^2 \omega_{1,2}^4 \ . \tag{5.20}$$

Substituting numerical values into Eq. (5.20) gives $\Delta\omega_1 = 0.67$ and $\Delta\omega_2 = 0.61$. Closer examination, however, reveals these numbers to be overestimates, because of evaluating Eq. (5.8) at the end points. More accurate matching of Eqs. (5.18) and (5.19) to Eq. (5.8) yields $\Delta\omega_1 = 0.17$ and $\Delta\omega_2 = 0.35$. Figure 5 is a schematic representation of $P(\omega)$ which exhibits its singularities at $\omega = 0$, ω_1, and ω_2. The intersections of the dashed lines illustrate the matching procedure just described.

We want now to present an alternative calculation of the curvature coefficient of Sec. III by integrating over the distribution of relaxation rates, as done by Koppel[12] for describing multicomponent diffusion. Because of the factor ω^2, the singularity shown in Fig. 5 at $\omega = 0$ disappears. In carrying out this integration we want to devote particular attention to the contributions at the end points. As explained above, these remaining singular contributions are confined close to the end points so that in these regions it is permitted to approximate ω^2 by its end-point values. The contribution of the singular part of the distribution at the lower end point becomes therefore

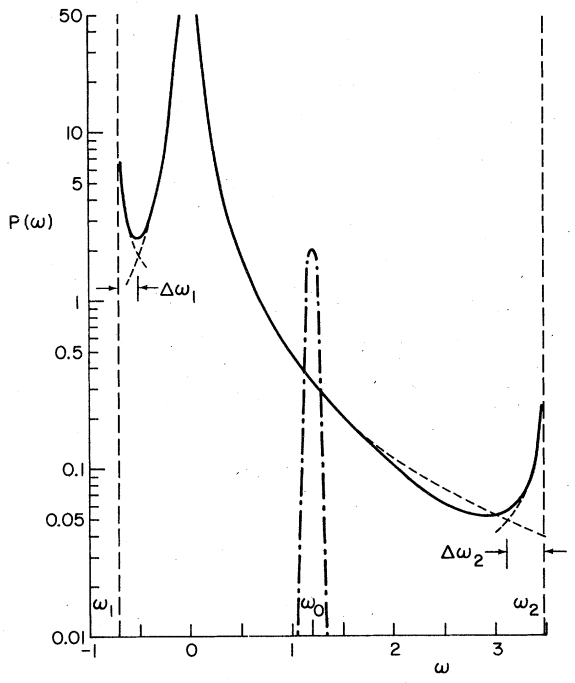

FIG. 5. $P(\omega)$, the relaxation rate distribution for double scattering, vs. $\omega = \Delta\Gamma/\Gamma_s$. The single scattering occurs at $\omega = 0$, also the location of the strong singularity in the double scattering, as shown. As is evident, $P(\omega)$ also has weaker singularities at the end points $\omega_1 = 0.69$ and $\omega_2 = 3.48$. The widths $\Delta\omega_1$ and $\Delta\omega_2$ describe the regions where the behavior of $P(\omega)$ is dominated by these end-point singularities. The δ function at $\omega_0 = 1.18$ leads to the correction factor shown as the dashed curve in Fig. 4.

$$\int_{\omega_1}^{\omega_1+\Delta\omega_1} d\omega\,\omega^2 P(\omega) \approx \omega_1^2 \int_{\omega}^{\omega_1+\Delta\omega} d\omega\,P(\omega)$$

$$= \omega_1^2 b_1 \int_{\omega}^{\omega_1+\Delta\omega} \frac{d\omega}{(\omega-\omega_1)^{1/2}}$$

$$= 2\omega_1^2 b_1 (\Delta\omega_1)^{1/2}$$

$$= 2\omega_1^2 \Delta\omega_1 P(\omega_1+\Delta\omega_1)$$

$$= 2\Delta\omega_1 (3/2\pi). \qquad (5.21)$$

A similar result holds at the upper end point. In deriving Eq. (5.21) we have written the integration in terms of the value of the distribution function at the boundary of the integration interval, $\omega_1+\Delta\omega_1$. The final step comes from the matching of Eq. (5.18) to Eq. (5.8). Equation (5.21) signifies that the singularity effectively doubles the contribution of the narrow interval of width $\Delta\omega_1$. This means that we can ignore completely the end-point singularities if we compensate by increasing the total interval of integration by $\Delta\omega_1$ and $\Delta\omega_2$ at the lower and upper ends, respectively. This gives

$$C_2 = \frac{1}{2}\int_{\omega_1}^{\omega_2} d\omega\,\omega^2 P(\omega) = \frac{1}{2}(\omega_2-\omega_1+\Delta\omega_1+\Delta\omega_2)\frac{3}{2\pi}$$

$$= \frac{(3/4\pi)}{4.69} = 1.12, \qquad (5.22)$$

5% larger than the value of 1.07 obtained from numerical integration. The magnitude of this error is comparable to that noted in Eq. (5.11) and is consistent with the accuracy of the approximations used.

The distribution of relaxation rates which has been discussed above and which is exhibited in Fig. 5 has a strong δ-function singularity at $\omega=0$ surrounded by a continuous distribution between the end points ω_1 and ω_2. The exact shape of this distribution is not directly accessible to experimental investigation. The shape of the distribution reveals itself through it various moments. The first moment results in a change in slope of the semilog plot of the intensity (see Fig. 6). The second moment corresponds to the curvature of the semilog plot. It is of interest to find the best fit that can be obtained by shifting the location of the strong central δ function by an appropriate amount away from $\omega=0$. Thus we try to fit the curved semilog plot by choosing a suitable straight line corresponding to a single exponential decay with a particular decay rate. In the frequency spectrum this would correspond to a pure Lorentzian shape. As the curvature that we are dealing with is $O(\epsilon)$,

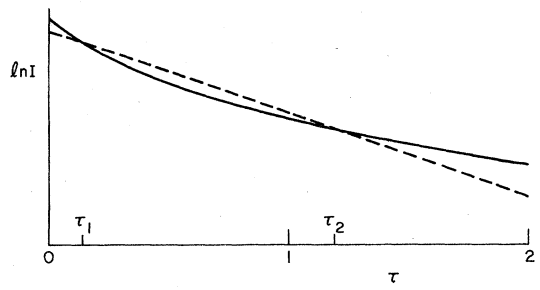

FIG. 6. Logarithm of $I(\tau)$, the time-dependent autocorrelation function of the electric field vs delay time. $I(0)$ is the mean intensity of the light reaching the detector. The curved semilog plot shown is a schematic representation of the effect produced by the mixing of the double-scattered light with the single-scattered light. τ is the delay time measured in units of the single-scattering relaxation time. The dashed line represents the best single-exponential least-squares fit to $I(\tau)$. This best fit produces a deviation plot with zeros at τ_1 and $\tau_2 = 0.14$ and 1.19, respectively.

it follows that we want to impose a fit on the function

$$I(\tau) = I_0 e^{-\tau}(1-\epsilon C_1\tau+\epsilon C_2\tau^2) \qquad (5.23)$$

with the "best-fit" choice of the simpler function

$$I_{BF}(\tau,\delta_0,\delta_1) = I_0 e^{-\tau}[1-\epsilon\delta_0 C_2+\epsilon(\delta_1 C_2 - C_1)\tau]. \qquad (5.24)$$

$\ln I_0$ is the sum of $\ln I_s$ and the $n=0$ term in Eq. (2.6). The parameters δ_0 and δ_1 will be chosen so as to minimize the mean square deviation. The deviation is given by the difference between Eqs. (5.23) and (5.24),

$$I(\tau) - I_{BF} = \epsilon C_2 I_0 e^{-\tau}(\delta_0 - \delta_1\tau+\tau^2). \qquad (5.25)$$

The minimization of the mean-square deviation

$$\delta\int_0^\infty d\tau\,[I(\tau)-I_{BF}]^2 = 0 \qquad (5.26)$$

is carried out with free variation of both parameters. This yields two linear equations with the solution

$$\delta_0 = \tfrac{1}{6}, \qquad (5.27)$$

$$\delta_1 = \tfrac{4}{3}. \qquad (5.28)$$

The deviation, although minimized for the time-dependent correlation function itself, is more easily visualized in terms of the deviation in the semi-

log plot. This deviation is represented by the parabola

$$\ln I(\tau) - \ln I_{BF} = \epsilon C_2(\delta_0 - \delta_1\tau + \tau^2)$$
$$= \epsilon C_2(\tau - \tau_1)(\tau - \tau_2) \tag{5.29}$$

with the roots

$$\tau_{1,2} = \tfrac{1}{6}(4 \pm \sqrt{10})$$
$$= 0.14, 1.19. \tag{5.30}$$

These roots are indicated schematically by the intersections of the dashed line representing $\ln I_{BF}$ with the curved semilog plot in Fig. 6.

It is also of interest to study the deviation from a pure Lorentzian in the frequency spectrum of the double-scattered light. For this it is convenient to return to the Taylor series expansion of Eq. (2.6) and to write it more formally as

$$d\omega\, P(\omega) e^{-(1+\omega)\tau}$$
$$= \int d\omega\, P(\omega)\left(1 + \omega\frac{\partial}{\partial\omega} + \frac{\omega^2}{2}\frac{\partial}{\partial\omega^2} + \cdots\right) e^{-(1+\omega)\tau}\Big|_{\omega=0}$$
$$= e^{-\tau}\int P(\omega)\, d\omega + \epsilon\left(-C_1\frac{\partial}{\partial\chi} + C_2\frac{\partial^2}{\partial\chi^2} + \cdots\right) e^{-\chi\tau}\Big|_{\chi=1}. \tag{5.31}$$

Here we have again introduced the moments of the relaxation-rate distribution function, as well as changing to the more convenient variable $\chi = 1 + \omega$. In terms of the frequency variable Ω (not to be confused with the relaxation rates ω and χ), the Fourier transform of a single exponential decay is

$$\{e^{-\chi\tau}\}_{FT} = L(\Omega, \chi) = (\chi/\pi)/(\chi^2 + \Omega^2). \tag{5.32}$$

Consequently the higher terms in Eq. (5.31), corresponding to distortions in the semilog plot, have the Fourier transforms

$$\left\{\frac{\partial}{\partial\chi}e^{-\chi\tau}\Big|_{\chi=1}\right\}_{FT} = \{-\tau e^{-\tau}\}_{FT}$$
$$= \frac{\partial}{\partial\chi}L(\Omega,\chi)\Big|_{\chi=1} = \frac{1}{\pi}\frac{\Omega^2 - 1}{(\Omega^2+1)^2} \tag{5.33}$$

and

$$\left\{\frac{\partial^2}{\partial\chi^2}e^{-\chi\tau}\Big|_{\chi=1}\right\}_{FT} = \{\tau^2 e^{-\tau}\}_{FT}$$
$$= \frac{\partial^2}{\partial\chi^2}L(\Omega,\chi)\Big|_{\chi=1} = \frac{2}{\pi}\frac{1 - 3\Omega^2}{(1+\Omega^2)^3}. \tag{5.34}$$

By applying Eqs. (5.33) and (5.34) to Eq. (5.25) we obtain the deviation as a function of frequency

$$\{I(\tau) - I_{BF}\}_{FT} = \epsilon C_2 I_0 \pi^{-1}\Delta(\Omega), \tag{5.35}$$

where

$$\Delta(\Omega) = \frac{\delta_0 + \delta_1}{1+\Omega^2} - \frac{2\delta_1}{(1+\Omega^2)^2} + \frac{2(1-3\Omega^2)}{(1+\Omega^2)^3}$$
$$= \epsilon C_2 I_0 \pi^{-1}\left(\frac{3}{2}\frac{1}{1+\Omega^2} - \frac{8}{3}\frac{1}{(1+\Omega^2)^2} + \frac{2(1-3\omega^2)}{(1+\Omega^2)^3}\right) \tag{5.36}$$

with roots at

$$\Omega_{1,2} = 0.39, 1.90. \tag{5.37}$$

$\Delta(\Omega)$ is shown in Fig. 7. It should be noted, by virtue of Parseval's theorem, that $\{I_{BF}\}_{FT}$ is the Lorentzian that is the best fit also in frequency space, in the least-mean-square sense, to $\{I(\tau)\}_{FT}$.

In the above we have seen that it is impossible to take into account the curvature of the semilog plot by simply shifting the central δ function. It is therefore of interest to see to what extent the curvature can be accounted for by using two δ functions. Some success in this direction has been reported by Beysens *et al.*[6] Such a representation of the continuum distribution of Fig. 5 can, of course, only be expected to be successful in a very limited context, at the best. As we are dealing with a strong δ function at $\omega = 0$ of $O(1)$, we can shift it so as to take into account a first moment of $O(\epsilon)$. The higher moments, however, thereby become of higher order in ϵ, and are negligible for our present purposes. In order to have a distribution which possesses higher moments, we need at least one more δ function of strength of $O(\epsilon)$, shifted by $O(1)$. This will give contributions of $O(\epsilon)$ to all higher moments, described by two parameters: the strength and position of the second δ function.

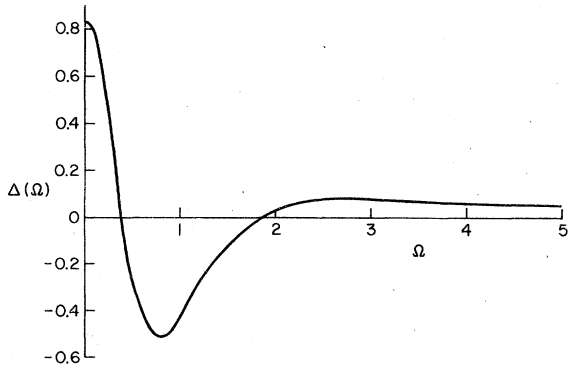

FIG. 7. Deviation of the spectrum of the double-scattered light from the best-fit Lorentzian. The frequency Ω is measured in units of the single-scattering relaxation rate Γ_s. The deviation $\Delta(\Omega)$ is defined in Eq. (5.36).

Including the shift of the central δ function, there is therefore in this approach a total of three parameters at our disposal. These can be determined by fitting to the first three moments. These moments correspond to the slope change and the curvature of the semilog plot of Fig. 6, as well as the initial slope of the plot of the correction factor in Fig. 4. The correction factor is obtained immediately from its basic definition and from Eq. (4.1). The latter reduces to an integration over the δ function indicated by the dot-dashed distribution at $\omega_0 = 1.18$ in Fig. 5. Thus, we obtain the explicit expression

$$F_\perp(\tau) = 2(e^{-\omega_0\tau} - 1 + \omega_0\tau)/(\omega_0\tau)^2 = 1 - \tfrac{1}{3}\omega_0\tau + \cdots , \quad (5.38)$$

which has been included in Fig. 4 as the dashed curve. It will be seen from this plot that, although the initial slope has been fitted correctly, the behavior at larger values of τ is completely different from the correct behavior shown by the solid curve. This indicates that representing the continuous distribution of the relaxation rates by only two δ functions, although providing a better fit than simply one δ function, is still too crude to describe all of the important features of the double scattering. Adding one more δ function, located at an appropriate negative value of ω would put two more parameters at our disposal and give us a much better fit to $F_\perp$. Such a representation, however, would seem to offer no advantage when, as in the present case, the correct continuous distribution, along with all of its moments, is already known.

VI. EQUAL-TIME CORRELATION FUNCTION

In this section we wish to make contact with the work of Bray and Chang[2] by calculating the same quantity which they did, namely, the total intensity of double scattering. In our preceding work, we have included the effect of dynamics and in our integrations there has been no sensitivity to the small angles. Therefore, we have been justified in working exactly at the critical point where the temperature parameter $\alpha = (k_0\xi)^{-1}$ has been set equal to zero. Now, however, when we turn to the intensity itself, we find that the extreme critical limit of $\alpha = 0$ leads to a divergent integral. We, therefore, consider a finite but very small value of α. The scattering tends to diverge when either $\Theta = 0$ or $\Theta' = 0$, in the notation of Sec. III A. As explained by Bray and Chang,[2] the contribution concentrated about $\Theta' = 0$ is equal to the contribution about $\Theta = 0$. For that reason we can limit our attention to integrating only in the vicinity of $\Theta = 0$ and multiplying the result by 2. The total intensity of the double scattering for perpendicular polarization is consequently

$$\epsilon_{\rm in}^{\perp} = B^2 \int_{-\infty}^{\infty} d\theta \int_{-h/2}^{h/2} dz \int_0^{r_0} \frac{r\,dr}{R^2}\,\frac{1}{\Theta^2+\alpha^2} . \quad (6.1)$$

In Eq. (6.1) we have made the small-angle approximation appropriate for $\alpha \ll 1$, which enables us to replace $\sin\frac{1}{2}\Theta$ by $\frac{1}{2}\Theta$. This also permits us to extend the integration from $-\infty$ to $+\infty$. The notation and the geometry is the same as that in Sec. III B, where we had to pay attention to the difference between R and r, the separations of the two scattering points in three-dimensions and in the x-y plane, respectively. This difference plays now, however, only a minor role, because of the small-angle scattering. Making a series of small-angle approximations, we transform the denominator of the integrand of Eq. (6.1) into

$$\begin{aligned} R^2\Theta^2 + R^2\alpha^2 &\approx R^2\Theta^2 + r^2\alpha^2 \\ &\approx x^2 + z^2 + r^2\alpha^2 \\ &\approx r^2\theta^2 + r^2\alpha^2 + z^2 \\ &\approx (\theta^2+\alpha^2)\left(r^2 + \frac{z^2}{\theta^2+\alpha^2}\right) . \end{aligned} \quad (6.2)$$

Carrying out the radial integration and ignoring the contribution of $\sec\theta \approx 1$, we find

$$\int_0^{r_0} \frac{r\,dr}{R^2}\,\frac{1}{\Theta^2+\alpha^2} \approx \frac{1}{\theta^2+\alpha^2}\int_0^{r_0} \frac{r\,dr}{r^2 + z^2/(\theta^2+\alpha^2)} = \frac{1}{\theta^2+\alpha^2}\ln\frac{r_0(\alpha^2+\theta^2)^{1/2}}{|z|} \quad (6.3)$$

provided $r_0 \gg h/2\alpha$ or $\gamma\alpha \gg 1$. Thus, with this additional restriction, independent cutoffs to the logarithm appear at both the upper and lower limits, as they did in Sec. III A. The lower cutoff comes about again because of the finite separation in the z direction of the two scattering points. Integrating out the z dependence in Eq. (6.3) gives the intensity as a function of the angle in the plane

$$\int_{-h/2}^{h/2} dz \int_0^{r_0} \frac{r\,dr}{R^2}\,\frac{1}{\theta^2+\alpha^2} = \frac{h}{\theta^2+\alpha^2}[\ln\gamma + \tfrac{1}{2}\ln(\theta^2+\alpha^2) + 1]. \quad (6.4)$$

For $\Theta \gg \alpha$, we can approximate Eq. (6.4) by $(h/\theta^2)\ln\gamma$. This is the approximation that was used in the first part of Sec. III A for the purpose of calculating the concavity in the semilog plot of the time-dependent correlation function. Later, in Sec. III B, we calculated the correction to $\ln\gamma$ by including various contributions which are important for the lower cutoff on the logarithmic integration. It is of some interest to calculate the correction to the logarithm by extending Eq. (6.4) beyond its range of validity and using it for large angles. Carrying out the integration over $\ln|\theta|$, we find a correction to $\ln\gamma$ of 0.58 as compared

with $c=0.13$ as calculated in III B. Besides the large-angle error, other effects, such as polarization factors different from unity, are responsible for this difference.

We now want to calculate the total intensity by carrying out the required integration over angle. For this we need the definite integral

$$\frac{1}{2}\int_{-\infty}^{\infty}\frac{d\theta}{\theta^2+\alpha^2}\ln\left(1+\frac{\theta^2}{\alpha^2}\right)=\frac{\pi}{\alpha}\ln 2. \tag{6.5}$$

Substituting Eqs. (6.5) and (6.4) into Eq. (6.1) yields

$$\epsilon_{\rm in}^{\perp}=\frac{\pi hB^2}{\alpha}(\ln\gamma+\ln\alpha+\ln 2+1)$$

$$=\frac{\pi hB^2}{\alpha}(\ln 2\alpha\gamma+1). \tag{6.6}$$

Equation (6.6) is identical to Eq. (3.25) of Bray and Chang.[2] The dimensional factors disappear when we consider, as they did, the ratio

$$R=\frac{\epsilon_{\rm in}^{\perp}}{\epsilon_{\rm out}}=\frac{1}{S(\alpha)}\frac{1}{\gamma\alpha}(\ln 2\alpha\gamma+1), \tag{6.7}$$

where we have substituted from Eq. (1.16). If we plot up this ratio we obtain curves such as shown in Fig. 2 of Bray and Chang,[2] depending upon the two variables α and γ. It is useful, however, to note that these various separate curves can be reduced to one "universal" curve if we plot instead the quantity $RS(\alpha)=\epsilon_{\rm in}/(\epsilon I_s)$. This gives us the function of only one variable

$$RS(\alpha)=(1/\gamma\alpha)(\ln 2\alpha\gamma+1). \tag{6.8}$$

With somewhat more labor, we can remove the restriction $\gamma\alpha\gg 1$ and carry out the calculation for arbitrary values of $\gamma\alpha$, provided only that $\gamma\gg 1$ and $\alpha\ll 1$. This yields

$$RS(\alpha)=\frac{1}{\gamma\alpha}\left(\frac{1}{2}\ln\frac{(1+\gamma^2\alpha^2)^{1/2}+\gamma\alpha}{(1+\gamma^2\alpha^2)^{1/2}-\gamma\alpha}+\gamma\alpha\sinh^{-1}\frac{1}{\gamma\alpha}\right), \tag{6.9}$$

which will be seen to reduce to Eq. (6.8) in the limit $\gamma\alpha\gg 1$. Equation (6.9) has been plotted vs. $\gamma\alpha$ as the solid curve in Fig. 8.

The remaining restrictions limit the applicability of Eq. (6.9) to large values of γ and small values of α. The former restriction is not serious, being compatible with the usual experiment arrangement. We can make use of the numerical calculations of Bray and Chang[2] to study the consequences of the latter restriction. Using their results, as exhibited in their Fig. 2, we have determined the deviation from "universality" for the two choices $\gamma=15$ and $\gamma=50$. These deviations are shown by the dashed curves in Fig. 8. They correspond to a 50% reduction in the value of RS at $\gamma\alpha=8$ and $\gamma\alpha=27$ for $\gamma=15$ and $\gamma=50$, respectively. Thus the deviation sets in at $\alpha\approx 0.5$, as expected. But in this range, although the percentage error in RS is large, the actual magnitude is small because R itself has become small. For this reason, we conclude that the universal function of Eq. (6.9) provides a convenient analytic as well as sufficiently accurate formula for RS for the entire range of α and for all values of γ no smaller than 15.

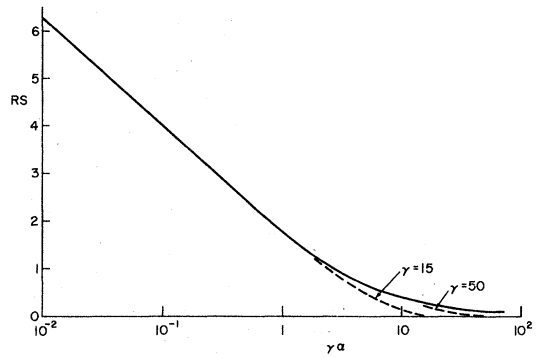

FIG. 8. Double-scattering intensity function RS vs $\gamma\alpha$. $R=\epsilon_{\rm in}/\epsilon_{\rm out}$, the ratio of the scattering-in to the scattering-out intensities. The scattering function $S(\alpha)$ describes the temperature variation of the turbidity, or alternatively of $\epsilon_{\rm out}$, and is defined in Eq. (1.15). $\alpha=(k_0\xi)^{-1}$, where k_0 is the wave number of the scattered light and ξ is the temperature-dependent correlation length. Small-angle approximations are permitted for $\alpha\ll 1$, and lead to the universal function of $\gamma\alpha$ shown as the solid curve. $\gamma=2r_0/h$, where r_0 and h are the radius and height of the scattering volume, respectively. The dashed curves are obtained from the numerical computations of Bray and Chang (Ref. 2) and indicate the deviation from the universal function resulting from finite values of α, where the small-angle approximations break down.

VII. SUMMARY

In the above we have found that the effect of double scattering is to cause the time dependence of the correlation function to be described by

$$\ln I=\ln I_0-(1+\epsilon C_1)\tau+\epsilon C_2\tau^2F(\tau). \tag{7.1}$$

In Sec. III and Appendix B, we have evaluated the moments of C_1 and C_2 in the extreme critical region by setting $\alpha=0$. In Appendix D, we have studied the variation of the curvature with α and this is exhibited in Fig. 9. In the case of $\perp$ polarization the numerical coefficients (see Secs. III A and III B and Appendix B are

$$C_1^{\perp}=-0.17\gamma^{-1}(\ln\gamma-2.2), \tag{7.2}$$

$$C_2^{\perp}=1.12\gamma^{-1}(\ln\gamma+0.13). \tag{7.3}$$

Similar results for $\parallel$ polarization are given in Sec. III C. The correction factors for $\perp$ and $\parallel$ polariza-

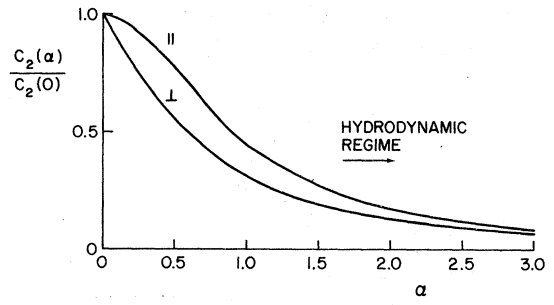

FIG. 9. Temperature dependence of the curvature for ⊥ and || polarization vs $\alpha = (k_0\xi)^{-1}$, where k_0 is the wave number of the scattered light and ξ is the correlation length.

tions are calculated in Secs. IV A and IV B, respectively, and are plotted versus τ in Fig. 4. The difference between I_0 and the single-scattering intensity I_s comes from the double scattering. This contribution has been calculated by Bray and Chang[2] and has also been reviewed by us in Sec. VI. We have noted there that the use of small-angle approximations, valid in the extreme critical regime $\alpha^{-1} = k_0\xi \gg 1$, greatly simplifies the calculation and leads to analytic results, as exhibited in Fig. 8.

The time variable τ is measured in units of the reciprocal of the relaxation rate for pure single scattering at 90°. The factor $1+\epsilon C_1$ in Eq. (7.1) coupled with the numerical value for C_1 given in Eq. (7.2) yields a change in the initial slope of the semilog plot of Fig. 6. On the other hand, the best fit of $I(\tau)$ to a single exponential-decay function is shown by the dashed line in Fig. 6. The slope of this line corresponds to a coefficient $1+\epsilon(C_1 - \delta_1 C_2)$ for the term of $\ln I(\tau)$ which is linear in τ. In Sec. V we found $\delta_1 = \frac{4}{3}$, so that the slope of the best-fit line is described by

$$1+\epsilon(C_1 - \delta_1 C_2) = 1.67\epsilon\gamma^{-1}(\ln\gamma - 0.11).$$

This correction factor should be divided into the best-fit slope in order to correct the latter for double scattering, and thereby convert it into the relaxation rate for pure single scattering, uncontaminated by double scattering. For example, for the parameter choice $\gamma = 50$ and $\epsilon = 0.10$, this correction amounts to a 1.3% increase in the rate; as remarked in Appendix B the dominant contribution comes from the curvature.

The above procedure is sufficient if the goal is to obtain a corrected value for the relaxation rate. But as discussed in Sec. I, there is theoretical reason to expect that even the single scattering will have a slight deviation from pure Lorentzian behavior. Experiments intending to reveal this deviation will require a comparison of Eq. (5.29) with the observed deviation of $\ln I(\tau)$ from the best straight line. Any disparity in this comparison will then be attributable to the single scattering. A more accurate and systematic approach, however, might avoid the assumption of an underlying straight semilog plot. Avoiding the best-fit approach, which tacitly ignores the expected frequency dependence, one could return to Eq. (7.1) and process the experimental data by subtracting the ϵ terms. Any residual curvature remaining in the semilog plot would then be a quantitative measure of true non-Lorentzian behavior of the single scattering.

APPENDIX A: SPATIAL COHERENCE OF DOUBLY SCATTERED LIGHT

The amplitude and intensity of the light incident at space-time point 1 on the photosensitive surface of the detector are $E(1)$ and

$$J(1) = E(1)^* E(1), \tag{A1}$$

respectively. With the usual Gaussian assumption for the fluctuations we consequently find for the correlation of the currents produced at two different points on the detector

$$\langle J(2)J(1)\rangle = \langle J\rangle^2 + |I(2,1)|^2, \tag{A2}$$

where the angular brackets denote the ensemble average over the scattering system. The second term in Eq. (A2) involves the correlation function for the electric field:

$$I(2,1) = \langle E(2)^* E(1)\rangle$$

$$= I_s(2,1) + I_D(2,1). \tag{A3}$$

The division of the intensity function into single- and double-scattering contributions is justified by the fact that the optical-path lengths for these two different modes of scattering differ by many wavelengths. There is therefore no interference between these two contributions. Let us first study the intensity function for the singly scattered light, which depends upon the electric field.

$$E_s(1) = \frac{\lambda}{r} e^{i(k_0 r_1 - \omega_0 t_1)} \int_s d^3r\, s(\vec{r}, t_1) e^{i\vec{k}_1\cdot\vec{r}}. \tag{A4}$$

λ is a coupling constant connecting the Maxwell field with the concentration (or density) fluctuation $s(\vec{r}, t_1)$, and is proportional to the polarizability of the molecules of the scattering medium. It connection with the constant B of Eq. (1.1) will be established presently. r_1 is the distance from the center of the scattering medium to point 1 of the detector. We assume that this distance is large compared with the dimensions of the scattering region. In this case the results are not sensitive to

the precise value of the prefactor r_1^{-1}. Therefore, in all subsequent work we replace r_1^{-1} by d^{-1}, where d is the distance between the center of the scattering region and the center of the detector. Furthermore, for the sake of simplicity, we assume that the photosensitive surface of the detector lies in the y-z plane, perpendicular to the line connecting the two centers. The general case is easily treated by only minor modifications. k_0 and ω_0 are the wave number (in the medium) and the frequency of the incident light, respectively. $\vec{k}_1$ is the difference between the initial and final wave numbers. The incident electric field has unit amplitude. t_1 is the arrival time of the light at point 1 of the detector. As we are interested in critical scattering, which occurs on a very much slowed-down time scale, we neglect the time of propagation from the scattering point to the detector. The integration is over the entire volume contributing to the single scattering, as denoted by the subscript s. Reference to Fig. 1 shows that this volume is defined in the y direction by the width of the exit slit $\Delta\omega$ and in the x and z directions by the beam dimensions.

In the problem under consideration the phase of the two separate terms in Eq. (A3) happens to be equal, which permits us to deal only with the absolute value of the correlation function. The phase factor appearing in front of the integral of Eq. (A4) thereby disappears and we find for the single-scattering correlation the double integral

$$|I_s(2,1)| = \frac{\lambda^2}{d^2}\left|\int_s\int_s d^3r'\,d^3r\, e^{i\vec{k}_1\cdot(\vec{r}-\vec{r}')} \times\langle s(\vec{r}',t_2)s(\vec{r},t_1)\rangle\right|. \quad \text{(A5)}$$

This integral in principle involves a six-dimensional integration over both three-dimensional variables $\vec{r}$ and $\vec{r}'$, each extending over the entire single-scattering region. The integration, however, is greatly simplified by the ensemble average, which defines the correlation function for the fluid

$$G(\vec{r}'-\vec{r},t_{21}) = \langle s(\vec{r}',t_2)s(\vec{r},t_1)\rangle, \quad \text{(A6)}$$

where $t_{21}=t_2-t_1$. For a correlation length small compared with the dimensions of the scattering region the variable $\vec{r}'$ is confined to a value relatively close to that of the variable $\vec{r}$. Its integration can therefore be carried out without reference to the boundaries of the scattering region and yields the Fourier transform of the correlation function

$$g(\vec{k},t_{21}) = \int d^3r e^{-i\vec{k}\cdot\vec{r}} G(\vec{r},t_{21}). \quad \text{(A7)}$$

The final integration yields

$$I_s(2,1) = (\lambda^2/d^2)g(\vec{k},t_{21})V_s\,|f_s(\vec{r}_{21})|, \quad \text{(A8)}$$

where V_s is the effective volume of the single-scattering region. The form factor determining the effect of spatial coherence[13] at the detector surface is

$$f_s(\vec{r}_{21}) = \frac{1}{V_s}\int_s d^3r\, e^{ik_0/d\vec{r}_{21}\cdot\vec{r}} a(\vec{r}), \quad \text{(A9)}$$

where $\vec{r}_{21}=\vec{r}_2-\vec{r}_1$ and $a(\vec{r})$ is the beam amplitude. The normalization of $f_s(0)=1$ requires $V_s \equiv \int d^3r\, a(\vec{r})$. Equation (A9) results from the fact that the momentum transfer for light arriving at two different points in the detector is slightly different. The difference is a vector lying entirely in the yz- plane and is equal to the angle of "tilt", r_{21}/d, times the wave number k_0. In the case of a point detector, $f_s(0)=1$, and Eq. (A8) reduces to a form which can be compared directly with Eq. (1.1). For this we need the Ornstein-Zernike expression for the equal-time correlation function,

$$g(k,0) = \frac{C}{k^2+\xi^{-2}} = \frac{C/k_0^2}{\alpha^2+4\sin^2\frac{1}{2}\theta}\,, \quad \text{(A10)}$$

where C is a particular constant of the fluid. In the case of a binary liquid it is a proportionality constant that occurs in the derivative of the concentration difference with respect to osmotic pressure. Multiplying by d^2 to obtain the scattering intensity per unit area and dividing by V_s to get the total amount of scattering per unit length (normalized to unit incident flux integrated across the beam) puts Eq. (A8) into the same form as Eq. (1.1) and enables us to identify the constant of proportionality occurring in Eq. (1.1) as

$$B = \lambda^2 C/k_0^2\,. \quad \text{(A11)}$$

Therefore the factor λ^2 which is being used in this analysis can be replaced, if desired by k_0^2B/C.

For the sake of definiteness we now present a few well-known expressions for f_s. The form factor that results from a simple rectangular-beam profile of overall vertical width $2w_B$ is

$$f_s^{\text{rect}}(y_{21},z_{21}) = \frac{\sin(k_0\Delta w/2d)y_{21}}{(k_0\Delta w/2d)y_{21}}\,\frac{\sin(k_0w_B/d)z_{21}}{(k_0w_B/d)z_{21}}\,. \quad \text{(A12)}$$

More common is a beam of circular cross section. For a beam of sharp profile and diameter $2w_B$, $a=1$ over the cross section and the form factor is found from an appropriate integration in the x-z plane (perpendicular to the beam axis) to be

$$f_s^{\text{cir}}(y_{21},z_{21}) = \frac{\sin(k_0\Delta w/2d)y_{21}}{(k_0\Delta w/2d)y_{21}}\,\frac{2J_1(k_0w_Bz_{21}/d)}{(k_0w_B/d)z_{21}}, \quad \text{(A13)}$$

where J_1 is the Bessel function. More realistic is a beam profile without any sharp boundary. Assuming a Gaussian falloff of the field strength away from the axis according to $a=\exp[-(x^2+z^2)/$

$w_d^2]$, we find

$$f_s^G(y_{21}, z_{21}) = \frac{\sin(k_0 \Delta w/2d) y_{21}}{(k_0 \Delta w/2d) y_{21}} e^{-(z_{21} k_0 w_B/2d)^2} . \tag{A14}$$

Because the slit width Δw plays the same role throughout, all three of the above expressions have the same y_{21} factor. Equation (A12) has an especially simple physical interpretation. Its dependence on y_{21} and z_{21} is identical to the y-z dependence (in the plane of the detector) of the Fraunhofer diffraction pattern produced by a slit of width Δw and height $2w_B$, located along the x axis a distance d from the detector, and illuminated by plane parallel light propagating in the x direction. The y and z dimensions of this diffraction pattern (i.e., distances between diffraction minima) are $4\pi k_0^{-1} d/\Delta w$ and $2\pi k_0^{-1} d/w_B$, respectively.

We now calculate the double scattering in a way similar to that done for the single scattering. Making the various approximations described above, we have for the doubly scattered electric field at point 1

$$E_D(1) = \frac{\lambda^2}{d} e^{i(k_0 r_1 - w_0 t_1)} \times \int\int \frac{d^3r' d^3r}{|\vec{r}' - \vec{r}|} e^{i\vec{k}_0 \cdot |\vec{r} - \vec{r}|} \times e^{ik_0 |\vec{r}' - \vec{r}|} e^{i\vec{k} \cdot \vec{r}} s(\vec{r}', t_1) s(\vec{r}, t_1). \tag{A15}$$

Proceeding now to calculate the intensity function for the double scattering leads to a fourfold integration over four different three-dimensional variables. In addition to the $\vec{r}$ and $\vec{r}'$ occurring in Eq. (A15), we have two more points to integrate over, say, $\vec{r}$ and $\vec{r}'$. The integrand contains the product of the four concentration (or density) fluctuations at these four points. But for a scattering region large compared with the correlation length, a contribution proportional to the square of the volume can come only from the pairwise factored form[14]

$$\langle s(\vec{r}', t_2) s(\vec{r}, t_2) s(\vec{r}', t_1) s(\vec{r}, t_1) \rangle = \langle s(\vec{r}', t_2) s(\vec{r}', t_1) \rangle \langle s(\vec{r}, t_2) s(\vec{r}, t_1) \rangle = G(\vec{r}' - \vec{r}', t_{21}) G(\vec{r} - \vec{r}, t_{21}) . \tag{A16}$$

[A similar argument justifies the Gaussian assumption used in deriving Eq. (A2).] Equation (A16) enables us immediately to dispose of the integrations over both $\vec{r}'$ and $\vec{r}$. The former brings in $\vec{k}'$, the momentum transfer at the first scattering and the latter brings in $\vec{k}$ the momentum transfer at the second scattering. The correlation function for double scattering is therefore the double integral

$$|I_D(2,1)| = \frac{\lambda^4}{d^2} \int\int \frac{d^3r' d^3r}{|\vec{r}' - \vec{r}|^2} g(\vec{k}', t_{21}) g(\vec{k}, t_{21}) |f_D(\vec{r}_{21})| , \tag{A17}$$

where the form factor for double scattering depends only upon the last scattering according to

$$f_D = \frac{1}{V_D} \int_D d^3r \, e^{i(k_0/d)\vec{r}_{21} \cdot \vec{r}} . \tag{A18}$$

With the given geometry the region of the second scattering is a tube along the x axis of constant rectangular cross section. f_D is consequently independent of x, which has permitted us to take it outside the integral. Equation (A18) is formally identical to Eq. (A9) for single scattering. They differ only in the region of the integration, which is now no longer limited by the beam dimension. The greater depth of the double-scattering region in the x direction is of no consequence, while the slit width in the y direction remains completely unchanged. The change in the z boundaries does, however, produce a modification. The overall height of the double-scattering region is h (see Fig. 1), which yields for the double-scattering form factor

$$f_D(y_{21}, z_{21}) = \frac{\sin(k_0 \Delta w/2d) y_{21}}{(k_0 \Delta w/2d) y_{21}} \frac{\sin(k_0 h/2d) z_{21}}{(k_0 h/2d) z_{21}} . \tag{A19}$$

Just as in the discussion above of Eq. (A12), Eq. (A19) corresponds to a diffraction pattern at the detector whose y and z dimensions are $4\pi k_0^{-1} d/\Delta w$ and $4\pi k_0^{-1} d/h$, respectively. Only when the detector dimensions are comparable to or greater than these does Eq. (A19) need to be taken into account. In general a numerical integration will have to be carried out. But the problem simplifies when the detector dimensions become much greater. Then all that we need from Eq. (A19) is the coherence area

$$A_D = \left(\frac{2\pi}{k_0}\right)^2 \frac{d^2}{\Delta w h} . \tag{A20}$$

The corresponding single-scattering coherence area from Eq. (A12) is

$$A_s^{\text{rect}} = (2\pi/k_0)^2 d^2/2\Delta w w_B . \tag{A21}$$

Therefore the correction factor in the large detector limit by which the double-scattering contribution to the correlation has to be renormalized relative to the single scattering, is

$$A_D/A_s^{\text{rect}} = 2w_B/h . \tag{A22}$$

The corresponding factors for the circular and Gaussian beams are

$$A_D/A_s^{\rm cir}=\tfrac{3}{16}\pi^2(w_B/h) \tag{A23}$$

and

$$A_D/A_s^{G}=\sqrt{\tfrac{1}{2}\pi}\,(w_B/h), \tag{A24}$$

respectively. As these three models for the beam profile represent successive reductions of the beam dimensions, the corresponding coherence areas which appear in the denominators of the left-hand sides of Eqs. (A22)–(A24) become successively larger. Consequently, the numerical coefficients appearing in the right-hand sides are in descending monotonic order. In actual practice, the height h is not greatly in excess of the beam width $2w_B$, so that the double-scattering normalization factors coming from Eqs. (A20)–(A24) do not result in a drastic reduction, even in the extreme-large-detector limit.[15]

APPENDIX B: CURVATURE AND SLOPE OF THE SEMILOG PLOT

We present here an exact evaluation of the second moment

$$C_2^{\perp}=\frac{1}{2\pi}\,\frac{\ln\gamma}{\gamma}\times\int_{-\pi/4}^{3\pi/4}\frac{(|\sin^3\tfrac{3}{2}\theta|+|\sin^3(\tfrac{1}{4}\pi+\tfrac{1}{2}\theta)|-1/2\sqrt{2})^2\,d\theta}{\sin^2\tfrac{1}{2}\theta\,\sin^2(\tfrac{1}{4}\pi+\tfrac{1}{2}\theta)}$$

$$=(1/2\pi)(\ln\gamma/\gamma)I_2,$$

where

$$I_2=\int_{-\pi/4}^{3\pi/4}\frac{|\sin^3\tfrac{3}{2}\theta|+|\sin^3(\tfrac{1}{4}\pi+\tfrac{1}{2}\theta|-1/2\sqrt{2})^2\,d\theta}{\sin^2\tfrac{1}{2}\theta\,\sin^2(\tfrac{1}{4}\pi+\tfrac{1}{2}\theta)}\,. \tag{B1}$$

In Sec. III, we calculated this integral by exploiting the virtual constancy of the integrand over the range of integration. That yielded $I=(\frac{9}{4})\pi$. It is convenient to expand the numerator and write

$$I_2=\int_{-\pi/4}^{3\pi/4}d\theta\left(\frac{\sin^4\tfrac{1}{2}\theta}{\sin^2(\tfrac{1}{4}\pi+\tfrac{1}{2}\theta)}+\frac{\sin^4(\tfrac{1}{4}\pi+\tfrac{1}{2}\theta)}{\sin^2\tfrac{1}{2}\theta}+\frac{1}{8}\,\frac{1}{\sin^2\tfrac{1}{2}\theta\,\sin^2(\tfrac{1}{4}\pi+\tfrac{1}{2}\theta)}-\frac{1}{\sqrt{2}}\,\frac{\sin(\tfrac{1}{4}\pi+\tfrac{1}{2}\theta)}{\sin^2\tfrac{1}{2}\theta}\right)$$

$$+\int_0^{\pi/4}d\theta\,2\sin\theta/2[\sin(\tfrac{1}{4}\pi+\tfrac{1}{2}\theta)+\sin(\tfrac{1}{4}\pi-\tfrac{1}{2}\theta)]+\int_{\pi/4}^{3\pi/4}d\theta 2\sin\tfrac{1}{2}\theta\sin(\tfrac{1}{4}\pi+\tfrac{1}{2}\theta)$$

$$-\int_0^{\pi}d\theta\,\frac{1}{\sqrt{2}}\sin\tfrac{1}{2}\theta\left(\frac{1}{\sin^2(\tfrac{1}{4}\pi+\tfrac{1}{2}\theta)}+\frac{1}{\sin^2(\tfrac{1}{4}\pi-\tfrac{1}{2}\theta)}\right)-\int_{\pi/4}^{3\pi/4}\frac{d\theta}{\sqrt{2}}\,\frac{\sin\tfrac{1}{2}\theta}{\sin^2(\tfrac{1}{4}\pi+\tfrac{1}{2}\theta)}\,. \tag{B2}$$

The advantage of writing the right-hand rule of Eq. (B1) in this form is the fact that the indefinite integral of each term can be evaluated. However, it is clear that some of the terms have a singularity at $\theta=0$, although the entire expression is well behaved. So, in integrating the terms which have such a singularity, we go from $-\frac{1}{4}\pi$ to $-\epsilon$ and from ϵ to $\frac{3}{4}\pi$, where $0<\epsilon\ll 1$. When all such terms are added, the parts which diverge as $\epsilon\to 0$ cancel, so that we can set $\epsilon=0$ and get a finite number for the integral. Using the following results,

$$\int d\theta\,\frac{\sin^4\tfrac{1}{2}\theta}{\sin^2(\tfrac{1}{4}\pi+\tfrac{1}{2}\theta)}$$

$$=\tfrac{1}{2}(\theta+\cos\theta)-\tfrac{1}{2}\tan(\tfrac{1}{4}\pi-\tfrac{1}{2}\theta)-\ln(1+\sin\theta),$$

$$\int d\theta\,\frac{\sin^4(\tfrac{1}{4}\pi+\tfrac{1}{2}\theta)}{\sin^2\tfrac{1}{2}\theta}$$

$$=\tfrac{1}{2}(\theta+\sin\theta)-\tfrac{1}{2}\cot\tfrac{1}{2}\theta+\ln(1-\cos\theta),$$

$$\int d\theta\,\frac{1}{\sin^2\tfrac{1}{2}\theta\,\sin^2(\tfrac{1}{4}\pi+\tfrac{1}{2}\theta)}$$

$$=4[\ln(1+\sin\theta)-\ln(1-\cos\theta)$$

$$-\tan(\tfrac{1}{4}\pi-\tfrac{1}{2}\theta)-\cot\tfrac{1}{2}\theta],$$

$$\int d\theta\,\frac{\sin(\tfrac{1}{4}\pi+\tfrac{1}{2}\theta)}{\sin^2\tfrac{1}{2}\theta}=\sqrt{2}\left(\ln\tan\tfrac{1}{4}\theta-\frac{1}{\sin\tfrac{1}{2}\theta}\right),$$

$$\int d\theta\,\frac{\sin\tfrac{1}{2}\theta}{\sin^2(\tfrac{1}{4}\pi+\tfrac{1}{2}\theta)}$$

$$=\sqrt{2}\left(\ln\tan\tfrac{1}{2}(\tfrac{1}{4}\pi+\tfrac{1}{2}\theta)+\frac{1}{\sin(\tfrac{1}{4}\pi+\tfrac{1}{2}\theta)}\right),$$

along with certain elementary trigonometric identities and integrals, we get

$$I_2=\pi+3\sqrt{2}+\pi/2\sqrt{2}+2\ln(\tan\tfrac{1}{8}\pi)$$
$$=\pi[1+3\sqrt{2}/\pi+1/2\sqrt{2}+(2/\pi)\ln(\tfrac{1}{8}\tan\pi)]$$
$$\simeq 2.14\pi. \tag{B3}$$

This gives

$$C_2^{\perp}=\frac{\ln\gamma}{\gamma}\frac{1}{2\pi}2.14\pi=1.07\frac{\ln\gamma}{\gamma}, \tag{B4}$$

which is 5% smaller than the value obtained from the linear approximation of Sec. III.

In studying the correction to the slope we find that the linear approximation is not sufficiently accurate. This can be understood from the plot of $\Delta\Gamma(\theta)/\Gamma_s$ in Fig. 3. The first moment depends upon a principal-value integration which is especially sensitive to the curvature at $\theta=0$. Furthermore the linear approximation neglects the "bulge" at larger values of θ. Therefore it is necessary to employ the above list of indefinite integrals to evaluate

$$\epsilon C_1^{\perp}=\epsilon\frac{\ln\gamma}{\gamma}\frac{1}{2\sqrt{2\pi}}$$
$$\times P\int_{-\pi/4}^{3\pi/4}d\theta\,\frac{|\sin^3\tfrac{1}{2}\theta|+|\sin^3\tfrac{1}{2}\theta+\tfrac{1}{4}\pi|-1/2\sqrt{2}}{\sin^2\tfrac{1}{2}\theta\sin^2(\tfrac{1}{4}\pi+\tfrac{1}{2}\theta)}$$
$$=\epsilon\frac{\ln\gamma}{\gamma}\frac{1}{2\sqrt{2\pi}}I_1, \tag{B5}$$

where

$$I_1=P\int_{-\pi/4}^{3\pi/4}d\theta\,\frac{|\sin^3\tfrac{1}{2}\theta|+|\sin^3(\tfrac{1}{4}\pi+\tfrac{1}{2}\theta)|-1/2\sqrt{2}}{\sin^2\tfrac{1}{2}\theta\sin^2(\tfrac{1}{4}\pi+\tfrac{1}{2}\theta)}$$
$$=F_P\Bigg(\int_0^{\pi/4}\frac{\sin\tfrac{1}{2}\theta\,d\theta}{\sin^2(\tfrac{1}{4}\pi-\tfrac{1}{2}\theta)}+\int_0^{3\pi/4}\frac{\sin\tfrac{1}{2}\theta\,d\theta}{\sin^2(\tfrac{1}{4}\pi+\tfrac{1}{2}\theta)}$$
$$+\int_{\pi/4}^{3\pi/4}\frac{\sin(\tfrac{1}{4}\pi+\tfrac{1}{2}\theta)}{\sin^2\tfrac{1}{2}\theta}d\theta$$
$$-\frac{1}{2\sqrt{2}}\int_{-\pi/4}^{3\pi/4}d\theta\,\frac{1}{\sin^2\tfrac{1}{2}\theta\sin^2(\tfrac{1}{4}\pi+\tfrac{1}{2}\theta)}\Bigg). \tag{B6}$$

Here the principal-value integration has been replaced by F_P, a "finite part" evaluation as explained above. This yields

$$I_1=2\sqrt{2}\,(\ln\tan\tfrac{3}{8}\pi-1/\sin\tfrac{1}{4}\pi), \tag{B7}$$

leading to

$$C_1^{\perp}=-0.17\epsilon\gamma^{-1}(\ln\gamma-2.2), \tag{B8}$$

where we have included an approximate calculation of the correction to the logarithm along the lines of Sec. III A. Numerical evaluation of this result reveals it to be a very small effect. For example, $\epsilon=0.10$ and $\gamma=50$ gives $\epsilon C_1^{\perp}=6\times10^{-4}$, in marked contrast to the second moment which is more than an order of magnitude larger.

The evaluation of the corresponding integrals for parallel polarization is simplified by the cancellation of the denominator by the polarization factor, as seen in Eq. (3.36). In this case the linear approximation proves to be reliable within the desired accuracy.

APPENDIX C: LARGE-τ NONLINEARITY

Here we present an alternative approach to Sec. IV A. The result obtained there is satisfactory for normal applications, but breaks down for very large values of τ. The advantage of the method that we now present is that it can be used in the range $\tau\gg1$. We define a function $G_{\perp}(\tau)$ by

$$(\ln I)_{\rm nl}=G_{\perp}(\tau)\epsilon(\ln\gamma)/\gamma. \tag{C1}$$

Using Eqs. (4.1), (3.4), and (3.6), we get

$$\frac{d^2G_{\perp}(\tau)}{d\tau^2}=\oint d\theta f(\theta)e^{-\Delta\Gamma/\Gamma_s\tau}$$
$$=f(0)\oint d\theta\,e^{-\Delta\Gamma/\Gamma_s\tau}$$
$$=\frac{9}{8\pi}\oint d\theta\,e^{-\Delta\Gamma/\Gamma_s\tau}$$
$$=\frac{9}{4\pi}\oint_{-\pi/4}^{3\pi/4}dr\,e^{-\Delta\Gamma/\Gamma_s\tau}. \tag{C2}$$

If we now use the linear approximation for $\Delta\Gamma/\Gamma_s$ to do the integration over angles in Eq. (B2) and then integrate twice over the time variable with the initial conditions $G_{\perp}(0)=dG_{\perp}/d\tau\big|_0=0$, we recover Eq. (4.9).

The linear approximation for $\Delta\Gamma/\Gamma_s$ is good over $0\leq\theta\leq\frac{3}{4}\pi$, but is not very accurate in the range $-\frac{1}{4}\pi\leq\theta\leq0$. $\Delta\Gamma/\Gamma_s$ is negative in this range. Because $\Delta\Gamma/\Gamma_s$ occurs in the integrand as $\exp(-\tau\Delta\Gamma/\Gamma_s)$, any error in $\Delta\Gamma/\Gamma_s$ in the range where it is negative becomes magnified for $\tau\gg1$. Therefore, we must find a better representation for $\Delta\Gamma/\Gamma_s$ in the interval $-\frac{1}{4}\pi\leq\theta<0$. This is provided by a parabolic approximation centered at $\theta=-\frac{1}{4}\pi$. It is convenient to define an angle ϕ by the relation

$$\phi=\theta+\tfrac{1}{4}\pi. \tag{C3}$$

A good fit is given in the two separate intervals by

$$\Delta\Gamma/\Gamma_s=\begin{cases}-0.69+1.26\phi^2 & \text{for } -\frac{1}{4}\pi\leq\theta\leq0\\ \text{or } 0\leq\phi\leq\frac{1}{4}\pi & \\ 3\theta/2 & \text{for } 0\leq\theta\leq\frac{3}{4}\pi.\end{cases} \tag{C4}$$

With this approximation, Eq. (B2) becomes

$$\frac{d^2G_\perp}{d\tau^2}=\frac{9}{4\pi}\left(\int_0^{\pi/4} e^{0.69\tau-1.26\tau\phi^2}\,d\phi + \int_0^{3\pi/4} e^{-3\tau\theta/2}\,d\theta\right). \tag{C5}$$

The second integration in the right-hand side of Eq. (C5) is trivial, while the first can be expressed in terms of the error function. The two further integrations required for obtaining $G_\perp(\tau)$ can be reduced to one integration. But in order to avoid the numerical task of integrating over the error function, we will be satisfied here to restrict ourselves to the asymptotic range $\tau \gg 1$. In this case the integrand of the first integral on the right-hand side of Eq. (C5) falls off very rapidly. This permits replacing the upper limit by infinity, giving

$$\frac{d^2G_\perp}{d\tau^2}=\frac{9}{4\pi}\left[\frac{1}{2}\left(\frac{\pi}{1.26}\right)^{1/2}\frac{e^{0.69}}{\sqrt{\tau}}+\frac{2}{3}\left(\frac{1}{\tau}-\frac{e^{-9\pi\tau/8}}{\tau}\right)\right]. \tag{C6}$$

Integrating twice yields

$$G_\perp(\tau)=\frac{9}{4\pi}\left(\frac{1}{2}\left(\frac{\pi}{1.26}\right)^{1/2}\left[\left(\tau+\frac{1}{1.38}\right)\int_0^\tau \frac{e^{0.69\tau'}}{\sqrt{\tau'}}\,d\tau'-\frac{\sqrt{\tau}}{0.69}e^{0.69\tau}\right] + \frac{2}{3}\left\{\tau\left[\ln\frac{9\pi\tau}{8}+C-1-Ei\left(-9\frac{\pi\tau}{8}\right)\right]+\frac{8}{9\pi}(1-e^{-9\pi\tau/8})\right\}\right)+K_0+K_1\tau, \tag{C7}$$

where $K_{0,1}$ are constants of integration and C (Euler's constant) $=0.577$. The remaining integral is a Dawson function. Imposing the boundary conditions on $G_\perp$ and its first derivative at $\tau=0$ would require $K_0=K_1=0$. This, however, makes tacit use of Eq. (C6) for small values of τ, outside the range of validity of this equation. Therefore, it is necessary to use the results from Sec. IV A. for specifying the boundary conditions at some intermediate compromise value of τ, say, $\tau_i=2.5$. This value of τ corresponds to where the curve in Fig. 4 for $F_\perp$ stops. The resulting values of $G_\perp(\tau)$ for $\tau>\tau_i$ lead to a correction factor defined by

$$F_\perp(\tau)=\tfrac{8}{9}G_\perp(\tau)/\tau^2. \tag{C8}$$

This function provides the appropriate extrapolation of Fig. 4 into the region $\tau>\tau_i$. Without this modified treatment, Eq. (4.11) would give an extrapolation which rises much too rapidly, for $\tau \gg \tau_i$, for reasons explained above.

APPENDIX D: TEMPERATURE DEPENDENCE OF THE CURVATURE

The curvature is given in the extreme hydrodynamic region by the integral of Eq. (3.5) where the integrand, using the linear approximation, can be replaced by its value at $\theta=0$ as exhibited in Eq. (3.11). This procedure holds in the extreme nonhydrodynamic limit, $\alpha \to 0$. When α takes on small but finite values, the denominator of $f_\perp(\theta)$ is the first to be modified and in the vicinity of $\theta=0$, $f_\perp(\theta)$ therefore acquires the correction factor

$$\theta^2/(\alpha^2+\theta^2)=1-\alpha^2/(\alpha^2+\theta^2). \tag{D1}$$

The negative term in the right-hand side of Eq. (C1) introduces a kind of "hole" in the integrand, whose effective width is given by the integration

$$\int_{-\infty}^{\infty}\frac{\alpha^2\,d\theta}{\alpha^2+\theta^2}=\pi\alpha. \tag{D2}$$

Here the use of small-angle approximations has permitted us to extend the limits of integration to infinity. In fact, however, there is a similar hole centered at $\theta=-\frac{1}{2}\pi$ so that the total effective width of the holes is $2\pi\alpha$ out of a total interval of 2π. Consequently, in the nearly extreme critical range, the curvature coefficient acquires the temperature dependence

$$C_2^\perp(\alpha)=C_2^\perp(0)(1-\alpha). \tag{D3}$$

We now turn to the hydrodynamic regime of $\alpha \gg 1$, where Eqs. (1.1) and (1.5) lose their angular dependence and become

$$I(\theta)=I_s=B/\alpha^2\,. \tag{D4}$$

Similarly, the distribution of the double-scattered intensity for perpendicular polarization loses its angular dependence and, instead of Eq. (3.2), acquires the constant value

$$\frac{dI_D^\perp}{d\theta}=\frac{hB^2}{\alpha^4}\ln\gamma. \tag{D5}$$

Consequently, the angular distribution that appears in the integration for the curvature coefficient, instead of having the angular dependence of Eq. (3.4), becomes the angle-independent dimensionless quantity

$$\frac{1}{\epsilon I_s}\frac{dI_D^\perp}{d\theta}=\frac{1}{2\pi\alpha^2}\frac{\ln\gamma}{\gamma}\,. \tag{D6}$$

The new equation replacing Eq. (3.6) for the integrand is, therefore, obtained from Eq. (D6) by including the appropriate factor from the dynamics and assumes the form

$$f_\perp(\theta) = (1/2\pi\alpha^2)(\Delta\Gamma/\Gamma_s)^2. \tag{D7}$$

Here the dynamics has to be modified in the hydrodynamic region. In place of Eq. (1.3) we have a quadratic dependence on wave number as described by

$$\Gamma(\theta) = \bar{\gamma}_s \sin^2\tfrac{1}{2}\theta, \tag{D8}$$

where the coefficient has a different value from the coefficient γ_s in Eq. (1.3). Substituting Eq. (D8) into the general form for $\Delta\Gamma$ gives us

$$(\Delta\Gamma/\Gamma_s)^2 = 2(1 + \sin\theta - \cos\theta - \sin\theta\cos\theta). \tag{D9}$$

Consequently, in the integration over angle, all of the terms except the first one in Eq. (C9) disappear, leaving

$$\oint f_\perp(\theta)\, d\theta = \frac{2}{\alpha^2}\,. \tag{D10}$$

Substituting now into Eq. (3.5) we have, for the temperature dependence of the curvature coefficient in the extreme hydrodynamic region

$$C_2^\perp(\alpha) = (1/\alpha^2)(\ln\gamma)/\gamma$$
$$= C_2^\perp(0)(8/9\alpha^2). \tag{D11}$$

A convenient Padé-type fit to the temperature dependence of the curvature coefficient which interpolates between the hydrodynamic and extreme nonhydrodynamic regions is

$$C_2^\perp(\alpha) = C_2^\perp(0)/(1 + \alpha + \tfrac{9}{8}\alpha^2)\,, \tag{D12}$$

as illustrated in Fig. 9. As is evident, the curvature rapidly becomes weaker as α increases. This is simply a consequence of the strong drop in double-scattering intensity when the system is taken away from the critical point. Consequently, curvature is observable mainly in the nonhydrodynamic regime.

The temperature dependence of the curvature for parallel polarization is different because the polarization factor $\sin^2\theta\cos^2\theta$ already produces "holes" at $\theta = 0$ and $-\frac{1}{2}\pi$. Consequently the correction factor of Eq. (C1) has little effect and there is no linear dependence of $C_2^\parallel(\alpha)$ on α in the vicinity of $\alpha = 0$. The appropriate Padé-type interpolation formula is therefore

$$C_2^\parallel(\alpha) = C_2^\parallel(0)/(1 + \tfrac{9}{8}\alpha^2)\,. \tag{D13}$$

[1]R. F. Chang, H. Burstyn, J. V. Sengers, and A. J. Bray, Phys. Rev. Lett. 37, 1481 (1976).

[2]A. J. Bray and R. F. Chang, Phys. Rev. A 12, 2594 (1975); see also L. A. Keith and H. L. Swinney, *ibid.* 12, 1094 (1975).

[3]R. A. Ferrell, Phys. Rev. 169, 199 (1968).

[4]C. M. Sorensen, R. C. Mockler, and W. J. O'Sullivan, Opt. Commun. 20, 140 (1977).

[5]D. W. Oxtoby and W. M. Gelbart, Phys. Rev. A 10, 738 (1974).

[6]D. Beysens and G. Zalcer, Phys. Rev. A 15, 765 (1977).

[7]V. G. Puglielli and N. C. Ford, Jr., Phys. Rev. Lett. 25, 143 (1970).

[8]R. Perl and R. A. Ferrell, Phys. Rev. Lett. 29, 51 (1972); Phys. Rev. A 6, 2358 (1972).

[9]L. S. Ornstein and F. Zernike, Proc. Acad. Sci. Amsterdam 17, 793 (1914); Z. Phys. 19, 134 (1918); 27, 761 (1926).

[10]K. Kawasaki, Ann. Phys. (N.Y.) 61, 1 (1970).

[11]R. Ferrell, Phys. Rev. Lett. 24, 1169 (1970).

[12]D. E. Koppel, J. Chem. Phys. 57, 4814 (1972).

[13]For discussions of the question of spatial coherence for single scattering see G. B. Benedek, in *Proceedings of Brandeis Summer Institute in Theoretical Physics*, 1966, edited by M. Chretien, E. P. Cross, and S. Deser (Gordon and Breach, New York, 1968), Vol. 2, pp. 1–98; and E. Jakeman, in *Photon Correlation and Light Beating Spectroscopy*, edited by H. Z. Cummins and E. R. Pike (Plenum, New York, 1974), pp. 75–150.

[14]This treatment differs from that of H. C. Kelly [J. Phys. A 6, 353 (1973)], who considers that the multiple scattering is produced by a large number of independent scatterers.

[15]This situation differs from that described by B. Volochine and P. Bergé [J. Phys. 31, 819 (1970)], who argue that $A_D/A_s \ll 1$ because of a much larger double-scattering volume.